

# PfSec13 is an unusual chromatin-associated nucleoporin of *Plasmodium falciparum* that is essential for parasite proliferation in human erythrocytes

Noa Dahan-Pasternak<sup>1</sup>, Abed Nasereddin<sup>1</sup>, Netanel Kolevzon<sup>2</sup>, Michael Pe'er<sup>1</sup>, Wilson Wong<sup>3</sup>, Vera Shinder<sup>4</sup>, Lynne Turnbull<sup>5</sup>, Cynthia B. Whitchurch<sup>5</sup>, Michael Elbaum<sup>6</sup>, Tim W. Gilberger<sup>7,8</sup>, Eylon Yavin<sup>2</sup>, Jake Baum<sup>3</sup> and Ron Dzikowski<sup>1,\*</sup>

<sup>1</sup>Department of Microbiology and Molecular Genetics, The Institute for Medical Research Israel-Canada, The Kuvim Center for the Study of Infectious and Tropical Diseases, The Hebrew University-Hadassah Medical School, Jerusalem 91120, Israel

<sup>2</sup>Institute for Drug Research, School of Pharmacy, Faculty of Medicine, The Hebrew University of Jerusalem, PO Box 12065, Jerusalem 91120, Israel

<sup>3</sup>Department of Infection and Immunity, Walter and Eliza Hall Institute of Medical Research, Parkville, VIC, 3052, Australia

<sup>4</sup>Electron Microscopy Unit, Weizmann Institute of Science, Rehovot 76100, Israel

<sup>5</sup>The ithree institute, University of Technology Sydney, Sydney, NSW, 2007, Australia

<sup>6</sup>Department of Materials and Interfaces, Weizmann Institute of Science, Rehovot 76100, Israel

<sup>7</sup>Department of Molecular Parasitology, Bernhard Nocht Institute for Tropical Medicine, 20359 Hamburg, Germany

<sup>8</sup>M.G. DeGrootte Institute for Infectious Disease Research, McMaster University, Hamilton, ON L8N3Z5, Canada

\*Author for correspondence ([rond@ekmd.huji.ac.il](mailto:rond@ekmd.huji.ac.il))

Accepted 24 April 2013

Journal of Cell Science 126, 3055–3069

© 2013. Published by The Company of Biologists Ltd

doi: 10.1242/jcs.122119

## Summary

In *Plasmodium falciparum*, the deadliest form of human malaria, the nuclear periphery has drawn much attention due to its role as a sub-nuclear compartment involved in virulence gene expression. Recent data have implicated components of the nuclear envelope in regulating gene expression in several eukaryotes. Special attention has been given to nucleoporins that compose the nuclear pore complex (NPC). However, very little is known about components of the nuclear envelope in *Plasmodium* parasites. Here we characterize PfSec13, an unusual nucleoporin of *P. falciparum*, which shows unique structural similarities suggesting that it is a fusion between Sec13 and Nup145C of yeast. Using super resolution fluorescence microscopy (3D-SIM) and *in vivo* imaging, we show that the dynamic localization of PfSec13 during parasites' intra-erythrocytic development corresponds with that of the NPCs and that these dynamics are associated with microtubules rather than with F-actin. In addition, PfSec13 does not co-localize with the heterochromatin markers HP1 and H3K9me3, suggesting euchromatic location of the NPCs. The proteins associated with PfSec13 indicate that this unusual Nup is involved in several cellular processes. Indeed, ultrastructural and chromatin immunoprecipitation analyses revealed that, in addition to the NPCs, PfSec13 is found in the nucleoplasm where it is associated with chromatin. Finally, we used peptide nucleic acids (PNA) to downregulate PfSec13 and show that it is essential for parasite proliferation in human erythrocytes.

**Key words:** Chromatin, Malaria, Nuclear pore complex, Nup, *Plasmodium falciparum*, Gene expression

## Introduction

In recent years increasing evidence has emerged that dynamics in nuclear organization contribute to the control of genome activity. Regulatory components of the transcriptional machinery were suggested to be located in discrete sub-nuclear compartments, creating 'transcriptional factories' in euchromatic regions (Chakalova et al., 2005). Upon activation, genes are localized to these sub-nuclear regions that are permissive for transcription while silent genes are located in regions that contain condensed heterochromatin (Egecioglu and Brickner, 2011; Takizawa et al., 2008). Special attention was given to the nuclear periphery as a sub-nuclear compartment, as it was shown that the NE is involved in the regulation of many nuclear processes including genome organization, epigenetics, transcription, splicing and DNA repair and replication (Zuleger et al., 2011). In many eukaryotes the nucleoplasmic region adjacent to the inner NE is

composed mainly of condensed heterochromatin and was shown to harbor silent genes and telomeres (Akhtar and Gasser, 2007). However, within this heterochromatic microenvironment the nuclear pore complexes (NPCs) define islands of loose genetic matter (Akhtar and Gasser, 2007; Arib and Akhtar, 2011; Capelson and Hetzer, 2009). It became clear that the NPCs are more than just a selective barrier between the nucleus and the cytoplasm but are also involved in the regulation of gene expression, chromatin organization and in maintenance of epigenetic memory (Blobel, 1985; Brickner and Walter, 2004; Cabal et al., 2006; Dieppois et al., 2006; Taddei et al., 2006; Tan-Wong et al., 2009). The NPC is composed of multiple copies of ~30 proteins, termed nucleoporins (Nups), which assemble to form one of the largest protein complexes in the cell (Grossman et al., 2012). The main components of this complex are the inner ring embedded in the NE, the cytoplasmic filaments and the

nucleoplasmic basket (Capelson and Hetzer, 2009). Some Nups located at the nuclear basket were shown to directly interact with DNA, chromatin and chromatin associated proteins (Arib and Akhtar, 2011; Capelson and Hetzer, 2009; Casolari et al., 2005; Ishii et al., 2002; Schmid et al., 2006; Tan-Wong et al., 2009).

In *Plasmodium falciparum*, the deadliest form of human malaria, the nuclear periphery was implicated in the regulation of expression of virulence genes. This protozoan parasite is responsible for over a million deaths a year (Aregawi et al., 2010) and its virulence was associated with its ability to evade the immune system through tight regulation of gene expression resulting in antigenic variation. Virulence genes in *P. falciparum* are located at the nuclear periphery (Freitas-Junior et al., 2000) and change their positioning upon changes in transcriptional status (Ralph et al., 2005) (Duraisingh et al., 2005; Freitas-Junior et al., 2005; Voss et al., 2006). In addition, active virulence genes such as *var* and *rif* genes co-localize to the same focus at the nuclear periphery (Dzikowski et al., 2007; Howitt et al., 2009; Joergensen et al., 2010) suggesting the existence of a specific expression site at this nuclear location. However, while the nuclear periphery was implicated in the regulation of virulence genes and epigenetic memory (Volz et al., 2012; Zhang et al., 2011), components of the NE and their possible involvement in the regulation of nuclear biology remains unknown in *Plasmodium* or any other apicomplexan parasite.

We have recently shown that changes in nuclear architecture during parasite development couple chromatin organization with changes at the nuclear envelope, particularly in the number and organization of the NPCs (Weiner et al., 2011). However, very little is known about components of the NPCs in these organisms. Computational search through the *Plasmodium* genome database (<http://plasmodb.org/plasmo/>) reveals very few orthologues to known Nups from other organisms (supplementary material Table S1). One of the interesting Nups that was identified is an orthologue to Sec13. This protein is conserved in most eukaryotes from yeast to mammals as an integral component of the NPCs. In addition, it is a component of the COPII-coated vesicle transport system in the cytoplasm. Sec13 is an essential Nup that plays a role in mRNA export, maintenance of the nuclear envelope and NPC integrity (Siniossoglou et al., 1996). In addition to its role as a component of the NPC, an episomal Sec13-GFP was also shown to be located in the nucleoplasm of mammalian cells (Enninga et al., 2003). Recently, certain Nups including Sec13 were shown to preferentially interact with chromatin at specific foci of *Drosophila* polytene chromosomes and were implicated in regulating gene expression (Capelson et al., 2010b; Kalverda et al., 2010; Vaquerizas et al., 2010).

In the current study we identified and characterized an unusual Sec13 orthologue in *P. falciparum* which we named PfSec13 (PFL1480w/PF3D7\_1230700, PlasmoDB.org ID). We found that PfSec13 is a larger protein than most eukaryotic Sec13 orthologues, with structural homology to the complex formed by ScSec13 and Nup145C. We created transgenic parasites and investigated the cellular dynamics of PfSec13 using super resolution microscopy (3D-SIM) and *in vivo* imaging. PfSec13 shows dynamic localization during parasite development, however, it does not co-localize with the heterochromatin markers HP1 and H3K9me3, suggesting a euchromatic location of the NPCs throughout the entire intra-erythrocytic cell cycle. In addition to the NPCs, we have found that PfSec13 associated with proteins involved in different cellular processes and is

located in the nucleoplasm where it is associated with chromatin. Finally, we show that PfSec13 is essential for parasites proliferation in human erythrocytes.

## Results

### An unusual Sec13 orthologue in *P. falciparum*

Sec13 maintains high level of conservation among evolutionarily distinct eukaryotes from yeast to humans. In most organisms the size of Sec13 is ~300 aa with several WD40 domains forming a  $\beta$ -propeller shaped protein (Brohawn and Schwartz, 2009; Stagg et al., 2006). Comparison of the amino acid sequence of the *P. falciparum* Sec13 orthologue (PfSec13, PFL1480w/PF3D7\_1230700, PlasmoDB.org ID) with that of several evolutionarily distinct eukaryotes indicated a high level of conservation in the first 376 aa of its N-terminus that contain the predicted WD40 domains (Fig. 1A) (Struck et al., 2008a). However, PfSec13 has an unusual extension and thus is predicted to give rise to a larger protein of 822 aa protein (90 kDa). As a first step we have aligned and compared the amino acids sequences of several *Plasmodium* species and found that *P. falciparum* and *P. knowlesi* encode large Sec13 proteins but *P. vivax* and the rodent malaria species *P. berghei* and *P. yoelii* lack this extension and encode only the shorter conserved region of Sec13 (supplementary material Fig. S1). At the NPC, Sec13 is a part of the Y shaped heptameric complexes, which are one of the core sub-complexes that compose the scaffold of the inner ring (Hoelz et al., 2011; Siniossoglou et al., 2000; Siniossoglou et al., 1996). In the yeast *Saccharomyces cerevisiae*, the molecular architecture of Nup84·Nup145C·Sec13 has been elucidated by crystallography revealing the structural association of the  $\beta$ -propeller Sec13 and Nup145C as well as the structural interaction of Nup145C and Nup84 (Brohawn and Schwartz, 2009). These data allowed us to perform *in-silico* structural prediction of PfSec13 based on its comparison to the complex structure of *S. cerevisiae* Sec13·Nup145C (Fig. 1B). As expected the conserved N-terminus of PfSec13 is predicted to form a  $\beta$ -propeller structure. However, while the N-terminus of PfSec13 has high similarity to ScSec13, the extension at the C-terminus shows high similarity to the structure of Nup145C. PfSec13 also contains three additional insertions that do not show homology to any other known proteins. The first insertion is located between amino acids 181 and 205, a longer second insertion is located between amino acids 595 and 629 and the third and longest insertion is located between amino acids 654 and 731. These insertions show no homology to any *Plasmodium* protein. Altogether, these data point towards a possible role of PfSec13 as a component of the NPC in *P. falciparum*.

### The nuclear dynamics of PfSec13 during *P. falciparum* development in human erythrocytes correspond with those of the NPCs

Previous 3D analyses of nuclear dynamics in *P. falciparum* showed that organization of the NPCs at the nuclear envelope undergoes significant changes during intra-erythrocytic development (IDC) involving clustering, biogenesis and division among daughter cells (Weiner et al., 2011). However, the lack of a molecular marker for NPCs made it difficult to study pore dynamics in detail and *in vivo*. Towards this aim, parasites were transfected with the expression plasmid pHSec13IDH-GFP in which PfSec13 was fused to GFP (supplementary material. Fig. S2). These parasites were used for both *in vivo* and high-resolution imaging using super resolution fluorescence microscopy (3D-SIM). In order to have precise

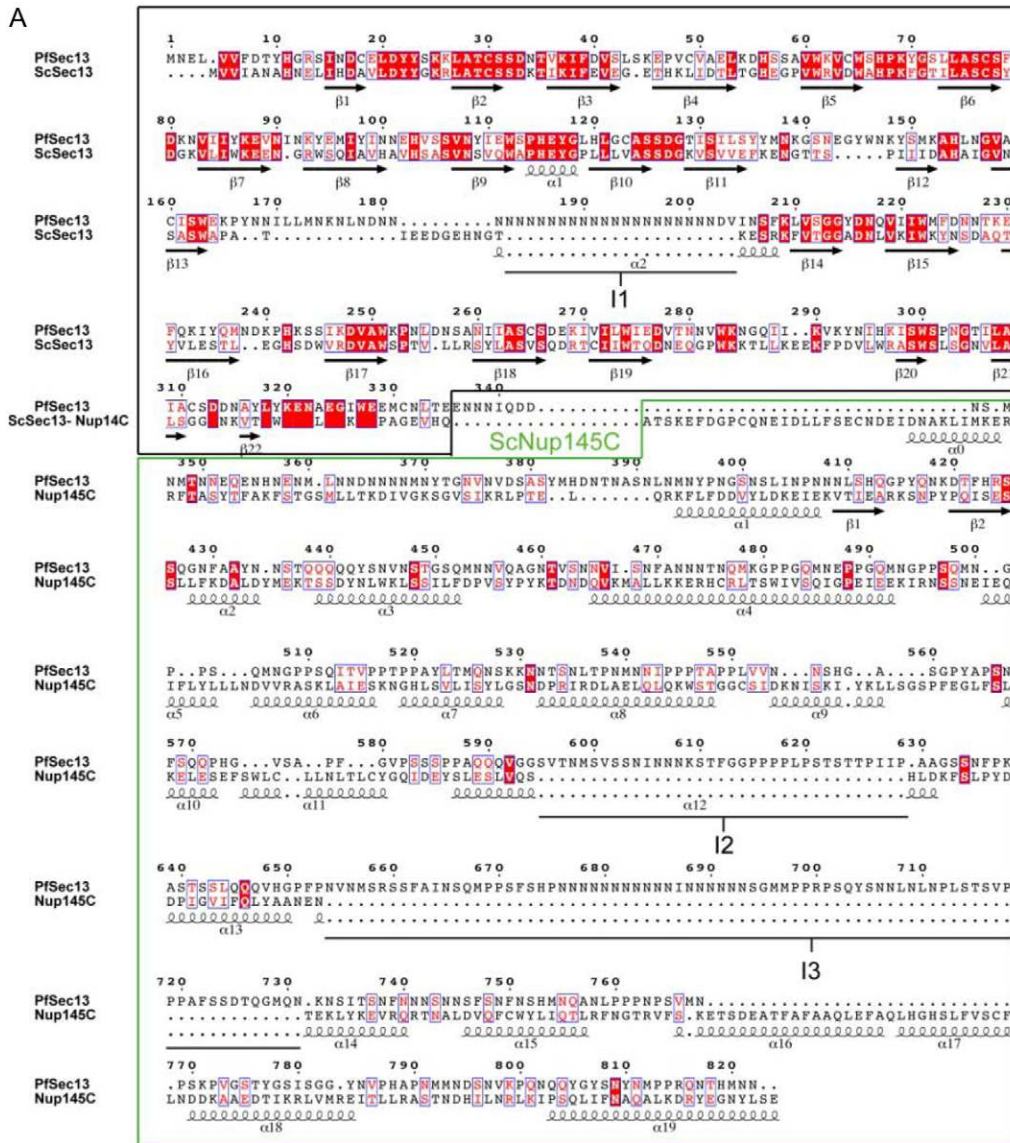


**Fig. 1. PfSec13 is a structural homolog of ScSec13-Nup145C.** (A) Structure-based sequence alignment of PfSec13 with ScSec13 and Nup145C. Residue numbering for PfSec13 is on top of the alignment. Secondary structural elements of ScSec13 are shown below the alignment. The  $\beta$ -propeller forming domain is indicated by the black box and the homology to Nup145C in the green box. Insertions specific to PfSec13 are labeled as I1–I3. Strictly conserved residues are highlighted by red shading. Homologous residues are highlighted in red text. (B) Overlay of the PfSec13 *in silico* model (purple) with crystal structure of ScSec13 (yellow; PDB code 3JRO) and Nup145c (green; PDB code 3JRO). The crystal structure of Nup84 is indicated in red (PDB code 3JRO).

temporal resolution of the different stages of development during the IDC, parasites were precisely synchronized by isolation of merozoites as recently described (Boyle et al., 2010). This method ensures that all parasites invade in a tight time window and allowed us to investigate in detail the cellular dynamics of PfSec13-GFP. Interestingly, using conventional fluorescence microscopy we could detect strong signals at the nuclear periphery and faint 'background' in the cytoplasm (Fig. 2A). However, when using super resolution microscopy we could differentiate between strong signals at the nuclear periphery and weaker signals seen in the cytoplasm (Fig. 2B; supplementary material Movie 1). Given the dual function of Sec13 as a Nup and as a component of the COPII coated vesicles, it is rational that the strong signals at the nuclear periphery correspond with NPCs clusters while the weaker cytoplasmic signals represent COPII vesicles. At the early phase of parasite development [10 min to 1 hpi (hour post invasion)] PfSec13-GFP seemed to be clustered at a distinct focus at the nuclear periphery. With the progression of the cell cycle the number of NPC signals increased, reaching a peak of 3.75 signals per nucleus (supplementary material Fig. S3) at 30 hpi. A closer look in high resolution at the signals at this stage indicated that they are clearly not round, suggesting that each of these signals represent a cluster of NPCs. During schizogony, as the number of nuclei increased the number of NPCs clusters gradually decreased to an average of 2.2 and 1.36 at 38 and 46 hpi, respectively

(supplementary material Fig. S3). In addition, in early schizonts (38 hpi) before cellularization of the daughter merozoites, most of the NPC clusters point outwards towards the cytoplasm of the mothers cell while in late schizonts each cluster points to a different direction (Fig. 2A) possibly to the cytoplasm of the new merozoites as we previously described (Weiner et al., 2011). *In vivo* imaging of PfSec13-GFP showed similar results (supplementary material Fig. S4). In addition, using known cellular markers to *Plasmodium* mitochondria, ER and Golgi we demonstrate that PfSec13 shows unique sub-cellular localization patterns (supplementary material Fig. S5). The patterns of cellular dynamics of PfSec13 observed here correspond with the dynamics of NPCs as observed by 3D electron microscopy reconstruction of *P. falciparum* nuclei (Weiner et al., 2011) supporting the role of PfSec13 as the first Nup described in *Plasmodium*.

### PfSec13 is associated with $\gamma$ -tubulin rather than with F-actin during IDC

Actin was shown to have important roles in parasite biology including processes such as motility, haemoglobin uptake and vesicular trafficking. In addition, recent advances that allow specific visualization of filamentous actin (F-actin) indicated that F-actin fibers concentrate at discrete zones at the nuclear periphery in early stages of parasite development (merozoites and rings) (Angrisano et al., 2012). F-actin was also implicated in

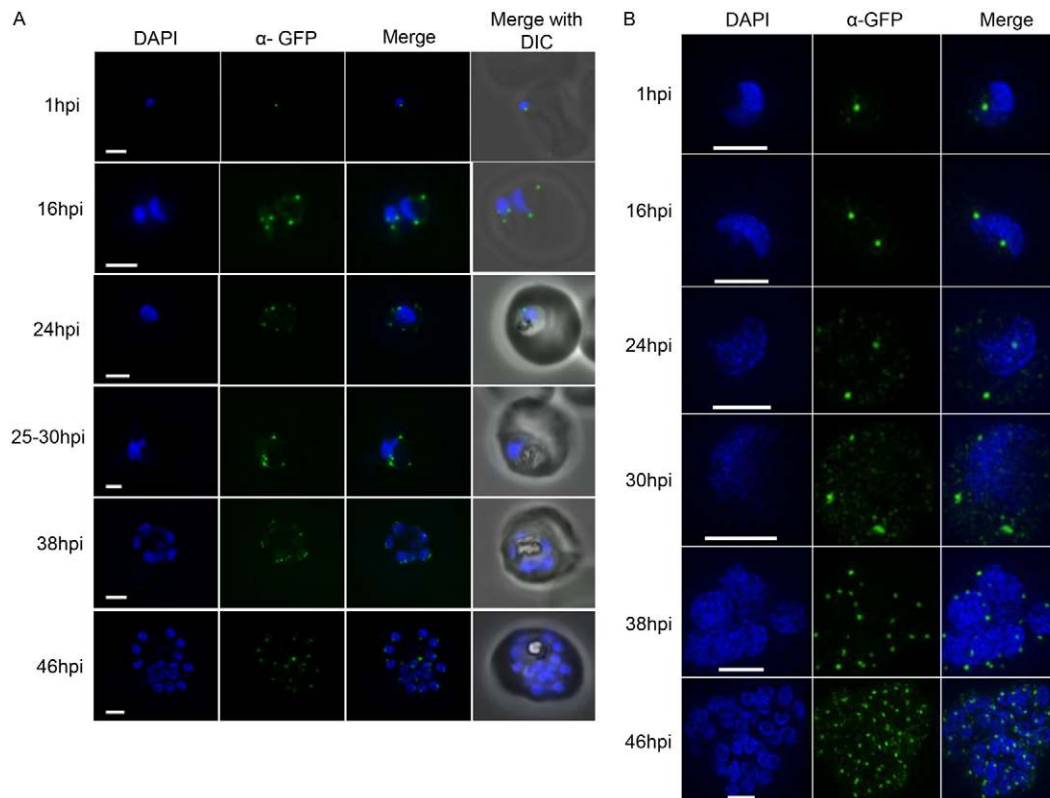


**Fig. 2. Dynamics of PfSec13-GFP during *P. falciparum* intra-erythrocytic development.** (A) Conventional fluorescent imaging of PfSec13-GFP (green) at different time points (hpi, hours post invasion) during the IDC. Strong signals of PfSec13-GFP at the periphery of the DAPI stained nucleus correspond with NPC clusters. Dynamics in cluster number and orientation were documented from 1 hpi to 46 hpi. At the late schizont stage (from 38 hpi to 46 hpi) there is a change in NPC orientation. Scale bars: 1  $\mu$ m. (B) High resolution microscopy (3D-SIM) of PfSec13-GFP showing an increase in the number of foci as parasites develop into trophozoites (1–30 hpi) and a gradual decrease during schizogony (36 and 48 hpi). The high resolution of these images enables differentiation between the large strong signals and the fainter ones. Scale bars: 2  $\mu$ m for 1, 16, 24, 38 and 48 hpi; 1  $\mu$ m for 30 hpi.

gene positioning at the nuclear periphery (Zhang et al., 2011) in early ring stages. In addition, in *S. cerevisiae* F-actin was found to be responsible for NPC dynamics (Steinberg et al., 2012). We were therefore interested to investigate the possible association between the nuclear dynamics of PfSec13 and F-actin throughout the entire IDC. We used the PfSec13-GFP parasites that enable co-localization of PfSec13 and F-actin using specific antibodies [ $\alpha$ -GFP and  $\alpha$ -Act<sub>239–253</sub> (Angrisano et al., 2012), respectively] and visualized the cellular dynamics of both proteins by 3D-SIM. We found that while in early merozoites and ring stages (10 min to 16 hpi) PfSec13 is associated with F-actin at the nuclear periphery (although they do not co-localize), later in the IDC PfSec13 remains located at the nuclear periphery while F-actin is

spread throughout the entire cell (Fig. 3A). In some fungal species, it was recently demonstrated that dynamics of NPC organization is mediated by F-actin while others use  $\gamma$ -tubulin as the main motor protein (Steinberg et al., 2012). We found that PfSec13 co-localized with  $\gamma$ -tubulin at different stages of development, in  $\sim$ 60% of the imaged nuclei (Fig. 3B,C). To further validate the possible association of PfSec13 with  $\gamma$ -tubulin we used a transgenic parasite line described below, in which PfSec13 was endogenously tagged with an HA epitope (Fig. 5A) and performed co-IP experiments. We found that while  $\gamma$ -tubulin co-precipitate with PfSec13, actin could not be detected in this fraction (Fig. 3D). The association of PfSec13 with  $\gamma$ -tubulin may indicate a possible role of microtubules in NPCs dynamics in *P. falciparum*.

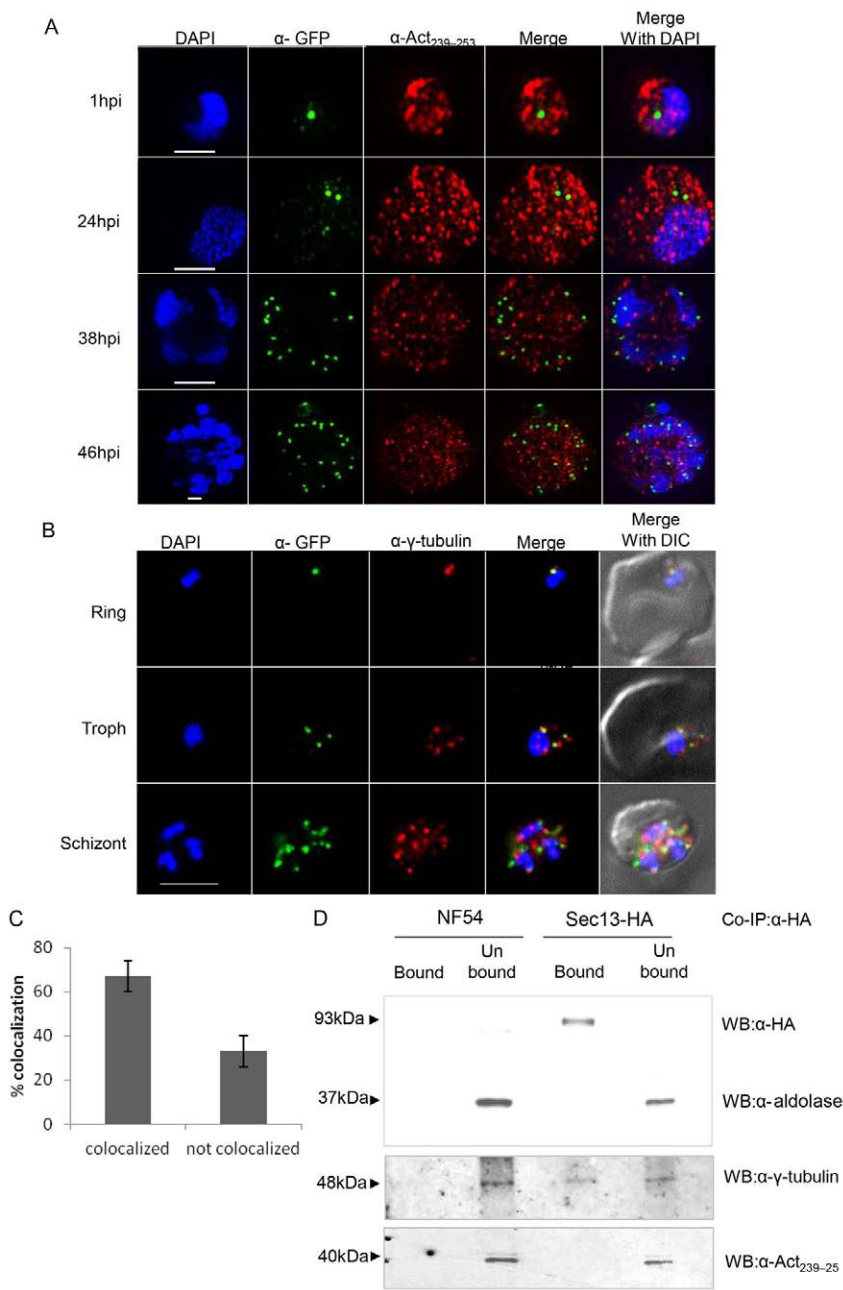


**Fig. 3. PfSec13 is associated with  $\gamma$ -tubulin rather than with F-actin.** (A) Super resolution IFAs of the PfSec13-GFP (green) expressing parasites that were co-stained with F-actin (red) using rabbit  $\alpha$ -Act<sub>239–253</sub> (Angrisano et al., 2012). Nuclei were stained with DAPI (blue). Scale bars: 1  $\mu$ m. (B) IFAs showing co-localization of PfSec13-GFP (green) and  $\gamma$ -tubulin (red) during the IDC. Scale bar: 5  $\mu$ m. (C) In  $\sim$ 60% of the 73 nuclei from all stages that were examined the NPCs were associated with  $\gamma$ -tubulin. (D) Western blot analysis demonstrating co-immunoprecipitation of  $\gamma$ -tubulin with PfSec13.  $\alpha$ -HA antibodies covalently bound to agarose beads were incubated with extracts from either asynchronous PfSec13-HA or NF54 parasite extracts. Western blot (WB) analysis using  $\alpha$ -HA antibodies indicated efficient PfSec13 IP ( $\sim$ 93 kDa), which is specific to the PfSec13-HA parasites (upper panel).  $\alpha$ -Aldolase antibody ( $\sim$ 37 kDa) was used as a loading control. The same membrane was then stripped and re-labeled with antibodies for  $\gamma$ -tubulin ( $\sim$ 48 kDa; middle panel) and F-actin ( $\alpha$ -Act<sub>239–253</sub>,  $\sim$ 40 kDa; lower panel).

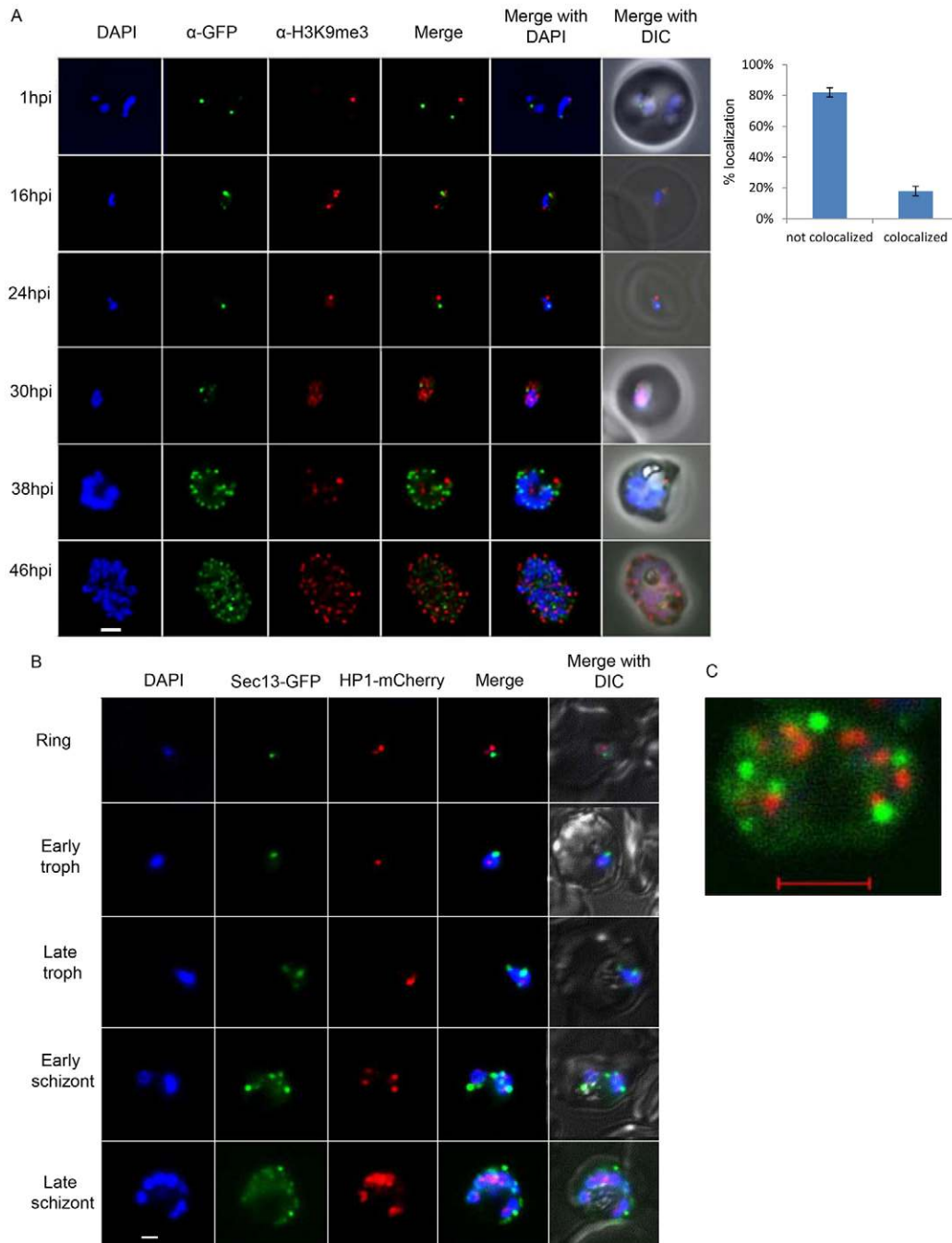


**Fig. 4. PfSec13 does not co-localize with *P. falciparum* heterochromatin.** (A) IFAs of the PfSec13-GFP expressing parasites that were co-immunolabeled with  $\alpha$ -GFP (green) and  $\alpha$ -H3K9me3 (red) at different stages of the IDC. In 85% of the counted nuclei of all stages ( $n=100$ ), the H3K9me3 signal and PfSec13-GFP did not co-localize (right-hand panel). Scale bar: 2  $\mu$ m. (B) *In vivo* imaging of parasites expressing both PfSec13-GFP and PfHP1-HA-mCherry (Flueck et al., 2009) during the IDC. Although PfSec13 (green) and PfHP1 (red) localized to the nuclear periphery they do not co-localize. Scale bar: 1  $\mu$ m. (C) *In vivo* confocal microscopy of parasites expressing both PfSec13-GFP and PfHP1-HA-mCherry. Scale bar: 2  $\mu$ m.

#### The NPCs of *P. falciparum* are found away from heterochromatin

The chromatin landscape of *P. falciparum* contains distinct heterochromatic regions within a generally euchromatic epigenome (Salcedo-Amaya et al., 2010; Trelle et al., 2009). Within this unusual epigenome heterochromatin is designated to be enriched with specific heterochromatin marks such as H3K9me3 and PfHP1 (Chookajorn et al., 2007; Lopez-Rubio

et al., 2009; Salcedo-Amaya et al., 2009). H3K9me3 and PfHP1 were shown to be associated with each other at distinct foci at the nuclear periphery (Flueck et al., 2009; Pérez-Toledo et al., 2009). In addition, these heterochromatin marks were implicated in silencing and epigenetic memory of virulence genes located at the nuclear periphery (Flueck et al., 2010). To determine if the NPCs in *P. falciparum* are found in euchromatic or heterochromatic regions we used the PfSec13-GFP parasite line

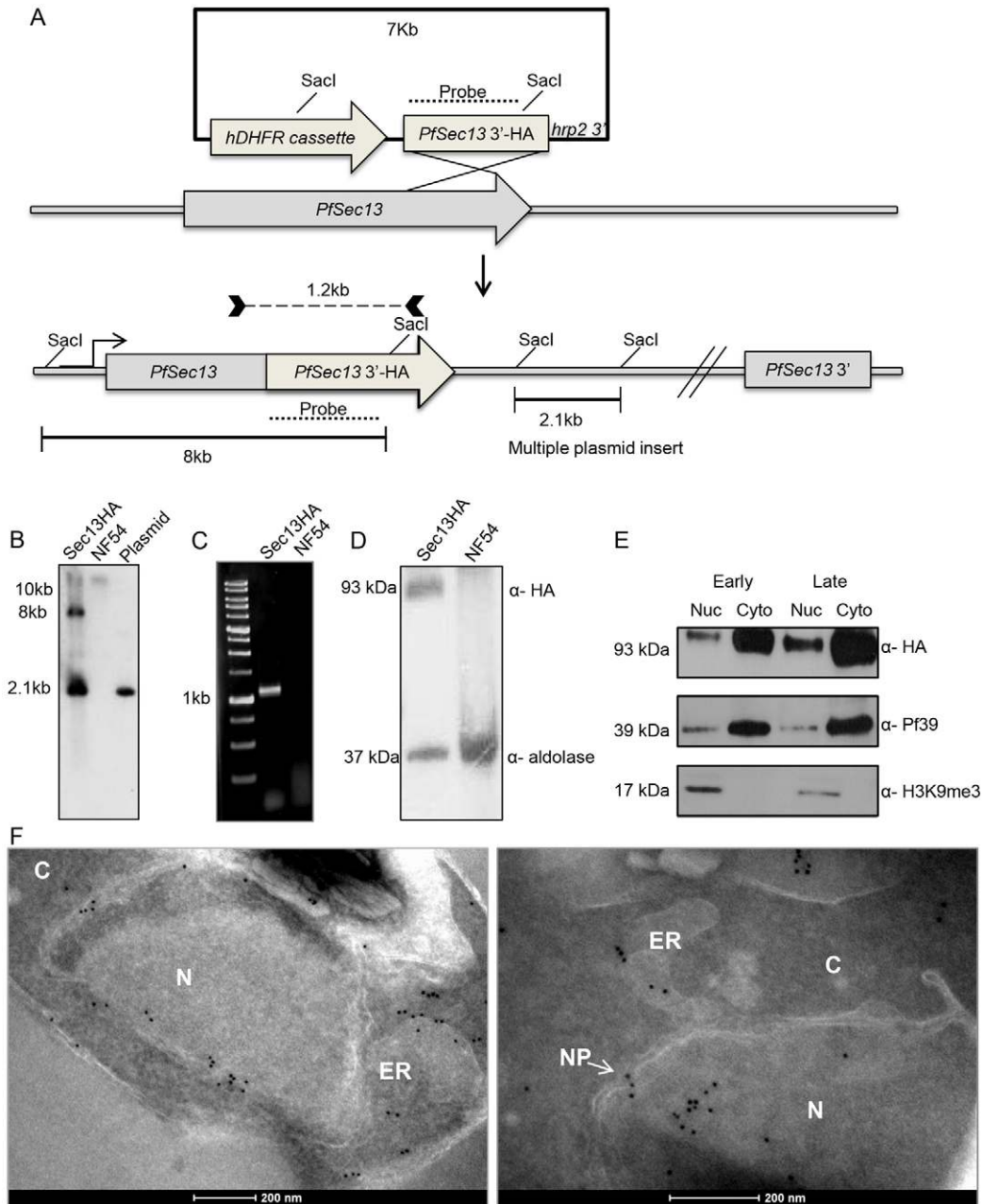


**Fig. 5. PfSec13 is found in the nucleoplasm in addition to the NPCs.** (A) PfSec13 was endogenously tagged with an HA epitope by 3' replacement. Schematic diagram showing the replacement of the PfSec13 3' end with 3 $\times$ HA from the construct pHSec13-3'-3 $\times$ HA by a single crossover recombination. The integration was confirmed by Southern blot (B). gDNAs from the transgenic PfSec13-HA and NF54 parasites as well as from the transfected plasmid (pHSec13-3'-3 $\times$ HA) were cut using *SacI* and probed with the *PfSec13* 3' fragment used on the plasmid. The location and sizes (8 kb and 2.1 kb) of the expected probed fragments are shown in A across the integration site and within the plasmid concatamer. NF54 parasites are expected to yield a 12 kb fragment and the plasmid only the 2.1 kb fragment. (C) PCR across the integration site gives a 1.2 kb amplicon specific to the PfSec13-HA parasites. Primer and amplicon location are shown as bold arrowheads and a dashed line, respectively, in A. The identity of this amplicon was confirmed by sequencing. (D) Western blot analysis of PfSec13-HA specific expression in the transgenic line yielding the expected 93 kDa band using  $\alpha$ -HA antibody while no band is shown in the NF54 parasites.  $\alpha$ -Aldolase antibody was used as loading control. (E) Cellular fractionation of the PfSec13-HA expressing parasite line, separating the cytosolic and nuclear content. The full length PfSec13-HA was detected by western blot in both the nuclear and cytosolic fractions in early and late developmental stages. (F) Immuno-EM of PfSec13-HA expressing trophozoites. PfSec13 localizes mainly to the nuclear envelope but gold particles can be also seen in the ER and cytosolic vesicles (left-hand panel). In some nuclei, PfSec13 is seen in the nucleoplasm (N) as well as in the nuclear pore (NP; white arrow) and the ER (right-hand panel). C, cytoplasm.

and performed immunofluorescence assays (IFAs) with specific  $\alpha$ -GFP and  $\alpha$ -H3K9me3 antibodies at different stages of IDC (Fig. 4A). We found that PfSec13 is found away from the heterochromatin marker H3K9me3 at all stages of parasite

development, indicating that PfSec13 localizes in euchromatic regions of the nuclear periphery. To confirm these findings we investigated the possible association of PfSec13 with PfHP1. We co-transfected the PfSec13-GFP parasite line with a vector

expressing PfHP1 fused to mCherry which enables *in vivo* visualization of both proteins within the same parasite. Similar to the results of the H3K9me3 co-localization experiment, we found that although PfSec13 and PfHP1 are often found adjacent to each other, they do not co-localize at any stage of the IDC, indicating again that PfSec13 is found away from heterochromatic regions of the nuclear periphery. Altogether the results of these experiments suggest that the NPCs in *P. falciparum* are located in euchromatic regions of the NE.

### PfSec13 is associated with chromatin in the nucleoplasm of *P. falciparum*

In addition to episomal expression of PfSec13 we created a transgenic parasite line (PfSec13-HA) in which the endogenous PfSec13 was fused with an HA epitope tag by 3' replacement (Fig. 5A). This line was created by transfecting p005-Sec13-HA plasmid (see Materials and Methods) into the DC-J parasite line (Dzikowski et al., 2006) and isolation of clonal populations in which the correct integration was confirmed by Southern blots, PCR and sequencing across integration site (Fig. 5B,C). Using western blot analysis with  $\alpha$ -HA antibody we were able to detect a specific single product at the expected size of 93 kDa (Fig. 5D) indicating that the tagged PfSec13 is expressed as a full length protein. The expressed PfSec13-HA was also visualized using IFA indicating that it is expressed during the entire IDC (supplementary material Fig. S5). In these experiments PfSec13-HA showed a similar dynamic organization at the NE as described above and did not co-localize with the ER marker Pf39. In addition, a one step cellular fractionation of parasite lysate revealed that PfSec13-HA is present within both the nuclear and cytoplasmic fractions (Fig. 5E). We further used this parasite line to determine the cellular localization of PfSec13 at the ultra structural level using immuno-EM with  $\alpha$ -HA antibodies. We found that PfSec13 is located at the nuclear envelope of trophozoite nuclei and that it clusters at the nuclear pore (Fig. 5F). PfSec13-HA is also present in the ER and in cytoplasmic vesicles, which is compatible with the cytoplasmic signals seen by super resolution microscopy and the known function of Sec13 as a component of the COPII coated vesicles. Interestingly, we observed that in many nuclei PfSec13-HA location is not restricted to the nuclear periphery but it is also found in the nucleoplasm (Fig. 5F, right-hand panel). These immuno-gold staining were specific to the HA epitope tag (supplementary material Fig. S6). We reasoned that in the nucleoplasm PfSec13 might be associated with chromatin. To test

this we used the PfSec13-HA transgenic line to perform chromatin immunoprecipitation (ChIP) using  $\alpha$ -HA antibody and measured IP enrichment by qRT-PCR. We found that several genes were clearly enriched in the IP fractions of PfSec13 compared with the mock antibody ( $\alpha$ -GFP) in the PfSec13-HA transgenic line and not in wt parasites in which PfSec13 was not fused to an epitope tag. Significant fold change in IP enrichment levels was observed in chromosomal loci that include subtelomeric (PFB1055c) and internal (PFD0630c) *var* genes as well as in the telomeric repeats regions (TARE). However, no significant enrichment was observed with HSP70 (PF08\_0054) and CSP (circusporozoite protein PFC0210c) (Fig. 6). This data suggests that PfSec13 is associated with particular chromosomal loci.

### PfSec13 is associated with proteins with variable cellular functions

In order to provide further evidence for the cellular roles of PfSec13, in addition to its role as a core NPC component, we were interested to identify its associated proteins. We performed co-IP experiments on the PfSec13-HA parasites using  $\alpha$ -HA antibody followed by mass spectrometry and compared the repertoire of the pulled down protein with co-IPs of NF54 parasites. The proteins which were recovered only in the transgenic PfSec13-HA parasites, or those that were significantly enriched in this line compared to the NF54 parasites are presented in Fig. 7A. As mentioned above (supplementary material Table S1) very few Nup homologues could be identified in *Plasmodium*. However, one of the proteins (PF3D7\_1423700) that was found to be specifically associated with PfSec13 contains a Nuclear Transport Factor (NTF) domain indicating that it might be associated with the NPC. Interestingly though, eight of the PfSec13 associated proteins are conserved among *Plasmodium* species but their function is unknown (Fig. 7A,B). It will be important to determine in the future if these contain additional components of *Plasmodium* NPC. In addition, PfSec13 is specifically associated with several RNA and DNA binding proteins including proteins implicated with transcriptional regulation (PF3D7\_1417200 and PF3D7\_0310500) and replication (PF3D7\_0409600), providing further support for their nucleoplasmic location and association with chromatin. The three proteins that together with Sec13 compose the coat complex of the COPII vesicles trafficking machinery were also associated with PfSec13 as expected. These data provide further support that PfSec13 is an unusual Nup with possible additional roles in the nucleoplasm as well as other cellular locations.

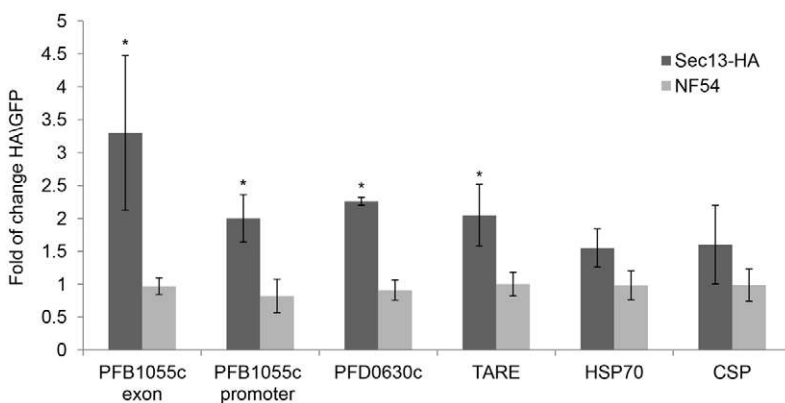


**Fig. 6. PfSec13 is selectively associated with chromatin.** ChIP was performed on PfSec13-HA parasites using  $\alpha$ -HA antibody. Data are presented as fold of change in enrichment using the  $\alpha$ -HA antibody and a mock  $\alpha$ -GFP antibody on PfSec13-HA parasites (dark columns) compared with the fold change in wild type NF54 parasites (light columns). Enrichment of specific chromosomal loci [a subtelomeric and internal *var* genes (PFB1055c and PFD0630c, respectively); Telomeric Associated Repeats, TARE; HSP70, PF08\_0054 and CSP PFC0210c] was measured by qPCR. The data represents the average and s.e. of at least three biological replicates. Significance was tested using a non-parametric Mann-Whitney *t*-test ( $P < 0.05$ ) and marked with asterisks.



**A PfSec13 associated proteins identified by LC-MS/MS.**

Cellular process	PlasmoDB ID	Annotation	Enrichment	
			Exp 1	Exp2
RNA/DNA binding	PF3D7_1224300	Polyadenylate-binding protein, putative.	*	2.8 fold
	PF3D7_0823200	RNA binding protein, putative.	*	*
	PF3D7_0923900	RNA binding protein, putative.	*	*
	PF3D7_1110400	Asparagine-rich antigen, (RRM -RNA recognition motif)	*	2 fold
	PF3D7_1409800	RNA binding protein, putative	*	5 fold
	PF3D7_1417200	NOT family protein, putative	*	5.4 fold
	PF3D7_0409600	Replication factor a protein, putative	*	5.5 fold
	PF3D7_0310500	DEAD box helicase, putative	*	2.6 fold
Nuclear transport	PF3D7_1423700	Conserved Plasmodium protein, unknown function (NTF2domain)	*	8 fold
	<b>PF3D7_1230700</b>	<b>protein transport protein Sec13, putative</b>	<b>8 fold</b>	<b>3.2 fold</b>
Translation	PF3D7_1312900	eukaryotic translation initiation factor 4 gamma, putative (EIF4G)	*	8 fold
Conserved, Unknown	PF3D7_0604500	Conserved Plasmodium protein, unknown function	*	*
	PF3D7_1119900	Conserved Plasmodium protein	*	4 fold
	PF3D7_0419400	Conserved Plasmodium protein, unknown function	*	3.5 fold
	PF3D7_1230800	Conserved Plasmodium protein	*	*
	PF3D7_1426800	Conserved Plasmodium protein, unknown function	*	5.5 fold
	PF3D7_0727900	Conserved Plasmodium protein, unknown function	*	11 fold
	PF3D7_0510100	Conserved Plasmodium protein, unknown function	*	16 fold
	PF3D7_0626000	Conserved Plasmodium protein, unknown function	*	*
COPII vesicle	PF3D7_0214100	Protein transport protein Sec31, putative	8.1 fold	7.2 fold
	PF3D7_0822600	Pfsec23:p , Pfsec23	5.1 fold	2.7
	PF3D7_0405100	Sec24-like protein, putative	*	5.5 fold
	PF3D7_0905900	Beta subunit of coatomer complex, putative	9 fold	4.6 fold
Invasion	PF3D7_0623100	Coronin binding protein	*	*
	PF3D7_1452000	PfRON2:p , rhostry neck protein 2	3 fold	3.6 fold
	PF3D7_1116000	RON4 moving junction protein	3.7 fold	6.6

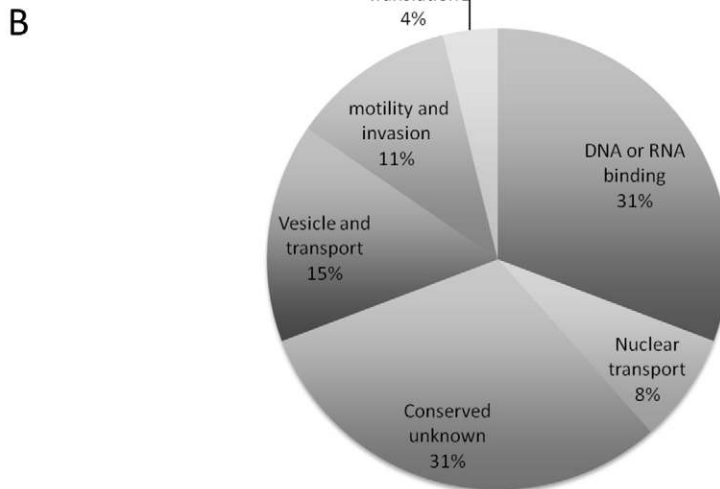


**Fig. 7. Proteins associated with PfSec13.** (A) List of proteins that were found to be associated with PfSec13-HA by LC-MS/MS analysis of two independent co-IP experiments (Exp1, Exp2). Proteins that were identified only in the PfSec13-HA co-IP but not in the negative control are marked with an asterisk. The fold enrichment is indicated for proteins that were enriched in the PfSec13-HA co-IP compared with the NF54 co-IP. (B) The proteins that were found to be associated with PfSec13 were sorted based on their predicted cellular functions. Most of the proteins are either DNA/RNA binding proteins (31%) or conserved proteins with unknown function (31%).

### PfSec13 is essential for *P. falciparum* proliferation in human RBCs

In yeast, Sec13 as well as other Nups in the Nup84 complex were shown to be essential proteins and their genetic deletion was

found to be lethal (Giaever et al., 2002; Siniouoglou et al., 1996). This might explain why we failed to recover transgenic parasites in which PfSec13 was genetically deleted (data not shown). In addition, inhibition of nuclear transport was found to be lethal

(supplementary material Fig. S7). Since the mechanism of gene knockdown by RNA interference does not exist in *Plasmodium* (Baum et al., 2009), in order to provide direct evidence that PfSec13 is an essential gene we decided to try a new methodology to downregulate PfSec13 using gene specific Peptide Nucleic Acid (PNA). PNAs are synthetic oligonucleotides with chemically modified backbones that can bind to both DNA and RNA targets in a sequence-specific manner (Wang and Xu, 2004). We synthesized a PNA molecule that complements the PfSec13 sequence and thus should specifically hybridize to the PfSec13 mRNA. In addition, we used a non-specific PNA molecule as negative control. The PfSec13-HA parasite line was incubated for 24 h with both specific and non-specific PNA molecules. After 24 h the culture medium was replaced daily (Fig. 8A). One generation post-incubation with 1.2  $\mu$ M PNAs, we obtained a specific 36.5% downregulation of PfSec13 in the parasite population that was incubated with the

PNA designed to hybridize to the coding region of *PfSec13*, while no effect was observed in those incubated with the control PNA (Fig. 8B, upper panel). We were also interested to test if downregulation of PfSec13 affects parasite viability. We used an NF45-*luc* parasite line in which the *luciferase* reporter gene is constitutively expressed and enables measurement of viability using simple *luciferase* assays (Salazar et al., 2012). These parasites were incubated with the 1.2  $\mu$ M of the same PfSec13-targeted and control PNA molecules. Interestingly, 48 h post incubation (insertion of the PNA molecules to the culture) we detected no difference in *luciferase* expression in parasites incubated with the PfSec13 PNA compared with the control (Fig. 8B, lower panel). However, one generation later, in parasites collected 96 h post incubation with the PNA molecules there was a decrease of almost 30% in *luciferase* expression between the two parasite populations. To confirm these results and obtain a stronger effect of the PNA we increased

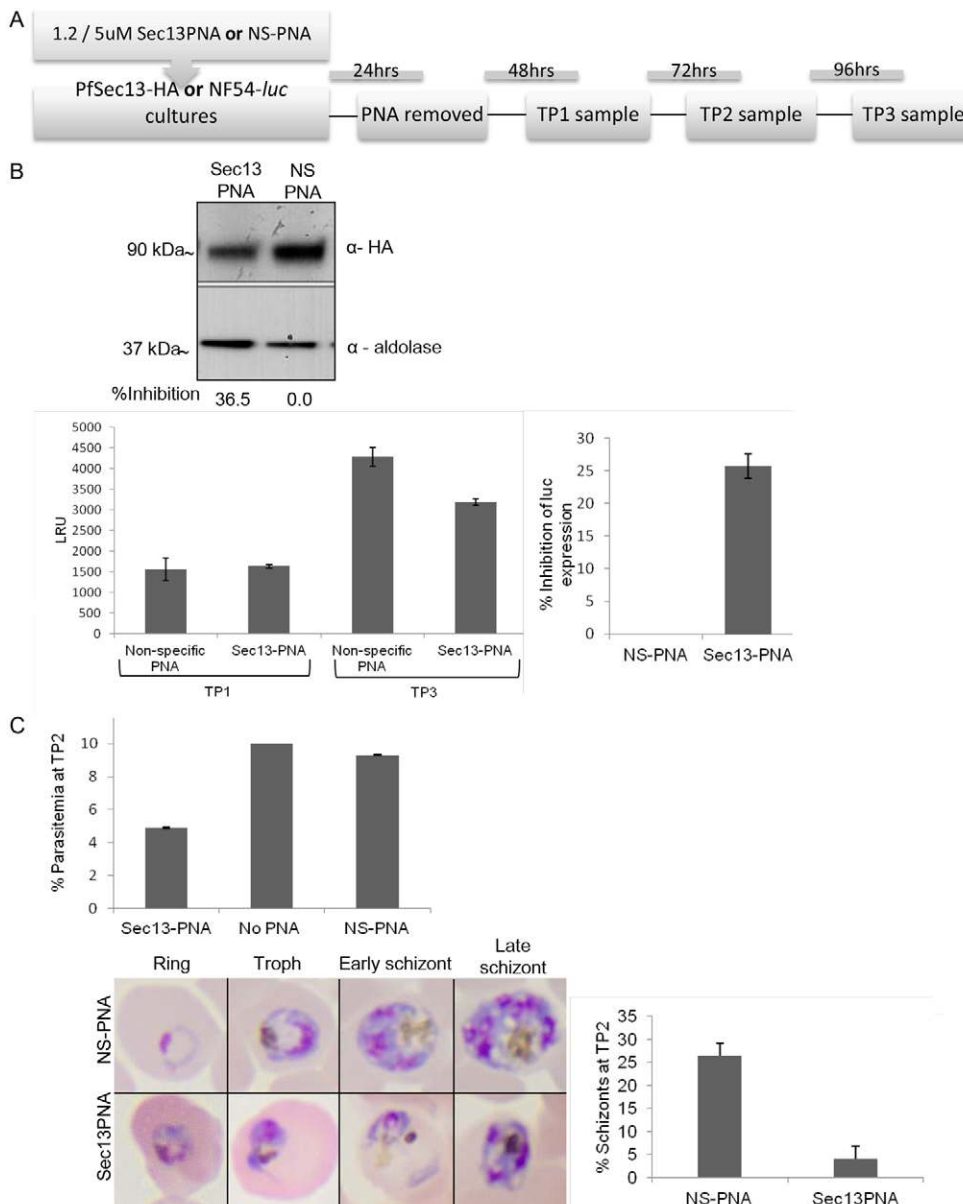


**Fig. 8. PfSec13 is essential for *P. falciparum* proliferation in human RBCs.** (A) Outline of experimental design. PfSec13-HA transgenic line or NF54-*luc* parasites that constitutively express the *luciferase* reporter gene were incubated with Sec13 specific (Sec13PNA) or non-specific PNA (NS-PNA) for 24 h. The PNA was then removed with culture medium and parasites were kept growing for an additional 24/72/96 h [time point (TP) 1, 2 and 3, respectively]. (B) PfSec13 is downregulated by specific PNA. Western blot analysis of parasites expressing the PfSec13-HA that were incubated with 1.2  $\mu$ M of either PfSec13 PNA or control non-specific (NS) PNA molecules, respectively. Expression levels of PfSec13 were reduced by 36.5% 48 h after incubation with the specific PNA (upper panel). Lower panel: downregulation of PfSec13 reduces the parasites' viability. NF54-*luc* parasites constitutively expressing the luciferase reporter gene were incubated with either PfSec13 PNA or control (NS) PNA, respectively. Parasites incubated with the specific PfSec13 PNA showed a 25.7% decrease in *luciferase* expression 96 h post incubation with 1.2  $\mu$ M PfSec13PNA. (C) Downregulation of PfSec13 alters parasite proliferation in human RBCs. Parasites incubated with 4.8  $\mu$ M PfSec13 PNA reached significantly lower parasitemia 72 h after incubation compared with control populations (upper panel). Lower panels: Giemsa stained blood smears showing normal development of parasites treated with 4.8  $\mu$ M non-specific PNA compared with parasites with deformation in cultures incubated with PfSec13 PNA 72 h post incubation. At this time point, this parasite population had a significantly lower amount of mature healthy schizonts. All experiments were performed in triplicate and the average is presented with s.e. LRU, luminescence rate unit.

its concentration to 4.8  $\mu\text{M}$ . 72 h post incubation with this concentration we obtained a significant decrease in parasitemia only in the parasite population incubated with the specific PfSec13-PNA (Fig. 8C, upper panel). Interestingly, many of the parasites in these cultures were deformed and almost no mature schizonts were observed in these cultures compared with the parasites populations that were incubated with the control PNA (Fig. 8C, lower panel). Altogether, this data indicates that downregulation of PfSec13 alters parasite proliferation in human RBCs.

## Discussion

In recent years the nuclear pore complexes are emerging as specialized sub-nuclear compartments which are involved in several nuclear functions such as transcription, splicing, genome organization and DNA repair (Arib and Akhtar, 2011; Capelson et al., 2010a; D'Angelo and Hetzer, 2006). The nuclear periphery of *P. falciparum* drew much attention as a sub-nuclear compartment, which is involved in virulence gene expression, however, to our knowledge components of the NE as well as the NPC were not thoroughly studied in these organisms. Here we identified and characterized PfSec13 as the first component of the NPC in *Plasmodium* with unique structural features. PfSec13 is a significantly larger protein than in other organisms which seems to evolve as a fusion that maintains the structural functions of the complex assembled by Sec13-Nup145C (or Nup107-160 in vertebrates) as part of the Nup84 complex, as well as its functions as a COPII component. In our hands, PfSec13 does not undergo processing and is found only in its large isoform as predicted by genome annotation. Whether additional Nups in *P. falciparum* have similar structural characteristics in which large Nups have structural similarities of two (or more) known Nups is yet to be determined. Interestingly, the extended feature of *Sec13* is also found in *P. knowlesi*, while other *Plasmodium* spp., in which *Sec13* was sequenced, have only the short conserved version of *Sec13*. The current knowledge on *Plasmodium* NPCs and COPII trafficking machinery makes it hard to speculate why such unique protein structures co-evolve specifically in *P. falciparum* and *P. knowlesi*. Further function structure analyses of *Plasmodium* nucleoporins and genome sequences of additional species could provide additional insight into the evolution of *Plasmodium* NPCs.

The dynamics of PfSec13 organization at the nuclear envelope during the IDC is similar to those of the NPCs. Using 3D model of *P. falciparum* nuclei we have recently shown that at early ring stages there are few NPCs that cluster together at one spot that corresponds with the strong single signal detected from PfSec13 at that stage. The number of NPCs per nucleus increases as the parasites' erythrocyte cycle progress reaches a peak in late trophozoites and decreases gradually during schizogony. In late schizonts when mature merozoites are ready to egress, one single spot is observed, corresponding with the NPC clusters seen at this stage (Weiner et al., 2011). Occasionally, we observe an NPC which seems to be pulled away from the nucleus into the cytoplasm. This phenomenon has been previously reported in yeast in which NPC motility involves nuclear extensions while maintaining the NE intact (Steinberg et al., 2012). Similar nuclear extensions were also reported in *P. falciparum* (Weiner et al., 2011). Furthermore, PfSec13 maintains specific cellular directionality similar to the clustered distribution of NPCs (Weiner et al., 2011). In early schizogony they face outward,

whereas in late schizonts they face the cytoplasm of each of the daughter merozoites, which is consistent with efficient transport of mRNA into the cytoplasm. Similar dynamics in the number and distribution of NPCs during the cell cycle were reported in certain plants and eukaryotes (Bucci and Went, 1997; Fiserova et al., 2009; Maeshima et al., 2006; Winey et al., 1997) (Colón-Ramos et al., 2003; Ho, 2010). In higher eukaryotes the NPCs are embedded in the nuclear lamina which is responsible for their organization, however, in lower eukaryotes such as *Plasmodium* there is no lamina and the mechanisms that are responsible for NPC dynamics are still elusive. Recently, it was demonstrated that motor driven ATP dependent movement is responsible for NPCs organization in several fungi (Steinberg et al., 2012). It was suggested that fungi constantly re-arrange their NPCs and corresponding chromosomes to overcome the need for nuclear lamina. Interestingly, NPCs movement in *Ustilago maydis* is driven by microtubules, kinesin-1 and dynein while in *S. cerevisiae* it is dependent on F-actin. Our results indicate an association of the NPCs with  $\gamma$ -tubulin in *P. falciparum* rather than association with F-actin. These data are in agreement with an early ultra-structure study that showed that microtubules form kinetic centers that interact with the cytoplasmic centrosome through the NPCs during closed mitosis in apicomplexan parasites (Schrével et al., 1977; Striepen et al., 2007). In addition, kinesin and dynein that are abundant in *P. falciparum* were shown to be associated with merozoite polarity (Fowler et al., 2001). Further studies are required to test the possibility that these motor proteins are involvement in regulating NPCs dynamics during IDC.

Considering the dramatic changes in chromatin organization during parasite development, it is interesting that the NPCs were found in regions of electron lucent genetic matter (Weiner et al., 2011). In agreement with our previous ultra-structural analysis our current data shows that NPC clusters are not located in regions that contain H3K9m3 and PfHP1, which were demonstrated as markers for silent heterochromatin in the unusual epigenome of *P. falciparum* (Chookajorn et al., 2007; Flueck et al., 2009; Lopez-Rubio et al., 2009; Pérez-Toledo et al., 2009; Salcedo-Amaya et al., 2009). These results are supportive of the 'gene gating' hypothesis proposed many years ago that the nonrandom distribution of NPCs at the nuclear periphery indicate that they can serve as a gating organelle capable of interacting specifically with transcribable portions in the genome (Blobel, 1985). Indeed, in addition to their role in nuclear transport, in recent years the NPCs were implicated in chromatin organization and gene expression (Akhtar and Gasser, 2007; Arib and Akhtar, 2011; Capelson and Hetzer, 2009; Köhler and Hurt, 2010). Active genes transcribed at the nuclear periphery were shown to interact with the NPCs (Schmid et al., 2006; Taddei et al., 2006) that function as chromatin boundaries that protect active promoters from the repressive effect of the neighboring heterochromatic environment of the nuclear lamina (Dilworth et al., 2005; Ishii et al., 2002). In addition to their role at the NPCs, several Nups including Sec13 were reported to be mobile and found within the nucleoplasm of higher eukaryotes (Daigle et al., 2001; Enninga et al., 2003; Enninga et al., 2002; Griffis et al., 2002; Lindsay et al., 2002; Powers et al., 1995; Rabut et al., 2004; Smitherman et al., 2000; Zimowska et al., 1997). Recent studies, investigating the role of Nups in the nucleoplasm, have demonstrated that Sec13 and additional Nups bind chromatin and are actively involved in regulating transcription in *Drosophila*

(Capelson et al., 2010b; Kalverda et al., 2010; Vaquerizas et al., 2010). Our finding that PfSec13 is selectively associated with chromatin in the nucleoplasm and is associated with several DNA and RNA binding proteins, is supported by recent analysis of the nuclear proteome of *P. falciparum* (Oehring et al., 2012). Using biochemical fractionation the sub-nuclear location of hundreds of nuclear proteins was determined. Interestingly, in addition to the membrane bound fraction, PfSec13 was also found in the sub-nuclear fraction that contains chromatin associated proteins. The presence of PfSec13 in the nucleoplasm of *P. falciparum* and its association with chromatin indicate a possible regulatory role in gene expression in lower eukaryotes as well.

In the cytoplasm, Sec13 function as a component of the COPII-coated vesicles that mediate transport from the endoplasmic reticulum (ER) to the Golgi apparatus. It is therefore reasonable that in addition to the nucleus PfSec13 was also present in the cytoplasmic fraction and detected by immune-EM in the ER and in cytoplasmic vesicles. Interestingly, episomes expressing a GFP fusion to the conserved 340 aa N-terminal part of PfSec13 that included the WD-40 repeat domains which forms the conserved  $\beta$ -propeller localized to defined sub-domains of the ER with dynamics similar to the Golgi (Struck et al., 2008a). Since the native PfSec13 is much larger and contains the domain which shares structural homology to Nup145C it is unclear where the truncated  $\beta$ -propeller part of the protein would bind and whether it could assemble into the Y complex of *Plasmodium* NPCs. Budding of the COPII vesicles requires the cytosolic assembly of the Sec13·Sec31 heterodimer that can polymerize into a cage that deforms the membrane and buds. *P. falciparum* contains an orthologue to Sec31 (PFB0640c) and one can speculate that the truncated N'-PfSec13-GFP forms a  $\beta$ -propeller that could assemble with the endogenous PfSec31 to form the COPII vesicles in the cytoplasm. However, considering the unique structure of the native PfSec13 it will be interesting to determine how COPII vesicles are forming in this organism.

The present study provides the first glance at components of the NPCs in *Plasmodium* unveiling the first Nup in this organism. Additional proteins, PFI0250c and PF14\_0706 were suggested as Nup candidates in *P. falciparum* and polyclonal antibodies that were raised against single peptides of each of these genes were used as nuclear periphery markers (Volz et al., 2010; Zhang et al., 2011). The inefficiency of the simple sequence analysis to identify Nups homologs in *P. falciparum* might indicate that some Nups could have evolved differently to function as more than one Nup as suggested for PfSec13 or that evolutionarily distinct organisms have different nucleoporin repertoires as was shown in plants (Tamura et al., 2010). The transgenic lines created here in which PfSec13 is endogenously tagged could be used to perform co-IP of the entire NPCs in order to unveil the entire Nup repertoire in *Plasmodium* similar to what was recently performed for African trypanosomes and *Arabidopsis* (DeGrasse et al., 2008; Tamura et al., 2010) which will provide valuable information about Apicomplexan NPC structure and function.

## Materials and Methods

### Parasite culture

All parasites used were derivatives of the NF54 parasite line, cultivated at 5% haematocrit in RPMI 1640 medium, 0.5% Albumax II (Invitrogen), 0.25% sodium bicarbonate and 0.1 mg ml<sup>-1</sup> Gentamycin (Sigma). Parasites were incubated at 37°C in an atmosphere of 5% oxygen, 5% carbon dioxide and 90% nitrogen. Percentage of infected erythrocytes was assessed by a blood smear that was methanol fixed and stained with Giemsa (Sigma).

### Structural and sequence homology for PfSec13

Structure-based sequence alignment of PfSec13 and ScSec13 was generated using Chimera 1.6.1 and Esript (Gouet et al., 1999; Yang et al., 2012). The PfSec13 model was generated using the I-TASSER server (Roy et al., 2010) and the figure was generated using PyMOL (Delano Scientific LLC, <http://www.pymol.org>). Sequence alignment of Sec13 across *Plasmodium* species was done using Clustal W and Esript (Chenna et al., 2003; Gouet et al., 1999).

### Immunofluorescence assay

IFA was performed as described before (Riglar et al., 2011) with slight modifications. Briefly, cells from a culture at 5% parasitemia were washed and re-suspended with fresh fixative solution (4% Paraformaldehyde (Sigma) and 0.0075% glutaraldehyde (EMS) in PBSx1). Fixed parasites were pelleted and treated with 0.1% Tx-100 (Bio-Rad) in PBSx1, then blocked with 3% BSA (Sigma) in PBSx1. Cells were then incubated with primary antibodies used at the following dilutions:  $\alpha$ -HA (Roche) 1/500, rabbit  $\alpha$ -H3K9me3 (Millipore) 1/300, mouse  $\alpha$ -GFP (Roche) 1/500, rabbit  $\alpha$ -Act<sub>239-253</sub> (Angrisano et al., 2012) 1/500, rabbit  $\alpha$ -gamma tubulin (Abcam) 1/500 and mouse  $\alpha$ -Pf39 (MR4) 1/500. Samples were washed and incubated with either Alexa-488<sup>®</sup> conjugated goat  $\alpha$ -mouse or Alexa-594<sup>®</sup> conjugated goat  $\alpha$ -rabbit secondary antibodies (Invitrogen). Samples were washed and settled on a Polyethyleneimine (Sigma) coated coverslips and mounted in VectaShield<sup>®</sup> DAPI stain. Fluorescence images were obtained using a Plan-Apochromat 100 $\times$ /1.40 oil immersion Phase contrast lens (Zeiss) on an AxioVert 200M microscope (Zeiss) equipped with an AxioCam Mrm camera (Zeiss). Z-stacks were processed using the Axiovision 4.8 deconvolution software package.

### In vivo imaging

The NF54 parasite line was co-transfected pBcamHP1-HA-Cherry (Flueck et al., 2009) and pH-Sec13-GFP-IDH. The culture was cultivated with double selection using 5 nM WR99210 and 2  $\mu$ g of blasticidin. Cells were pelleted, diluted with 1 $\times$  PBS and incubated with Hoechst 33342 fluorescent stain (Thermo Scientific). Then samples were laid on a Teflon coated slide (EMS), covered with 18 $\times$ 18 cover slides and immediately visualized. Images were taken using Apochromat oil immersion objective with  $\times$ 100 magnification (Olympus) on an Olympus IX71S8F microscope equipped with Exi Blue<sup>™</sup> Fast camera (QImaging).

### Super resolution optical imaging

Samples were prepared for IFA and visualized in a DeltaVisionOMX 3D Structured Illumination Microscopy System<sup>®</sup> (OMX 3D-SIM, Applied Precision Inc., Issaquah, USA), as described previously (Riglar et al., 2011).

### Immuno EM

Parasites were fixed in 4% paraformaldehyde with 0.1% glutaraldehyde in 0.1M cacodylate buffer (pH=7.4), for 1 hour at room temperature and kept at 4°C for 1–2 days. The samples were soaked overnight in 2.3M sucrose and rapidly frozen in liquid nitrogen. Frozen ultrathin (70–90 nm) sections were cut with a diamond knife at –120°C on a Leica EM UC6 ultramicrotome. The sections were collected on 200-mesh formvar coated nickel grids. Sections were blocked by a blocking solution containing 1% BSA, 0.1% glycine, 0.1% gelatin and 1% Tween 20. Immunolabeling was performed using mouse  $\alpha$ -HA antibody (1:100; Roche) for 1.5–2 hours at room temperature followed by goat anti-mouse IgG coupled to 10-nm (or 15 nm) gold particles (1:20 dilution) 30 min at room temperature. Contrasting and embedding were performed by Tokuyasu (Tokuyasu, 1986). The embedded sections were scanned and digitally viewed on transmission electron microscope Tecnai Spirit (FEI) at 120 kV using CCD Eagle camera with TIA software (FEI).

### Fractionation

Fractionation was done as described before (Flueck et al., 2009). Briefly, saponin lysed parasites were re-suspended with cell lysis buffer (CLB) incubated on ice for 30 minutes and pelleted. The supernatant was kept as the cytosolic fraction and the pellet was washed with CLB until clear and then kept as the nuclear fraction. Each fraction was analyzed by SDS-PAGE and western blot as described. The relative intensity of the bands of nuclear and cytosolic fractions was assessed by ImageJ (Rasband, W.S., ImageJ, US National Institutes of Health, Bethesda, Maryland, USA, <http://rsb.info.nih.gov/ij/>, 1997–2009).

### SDS-PAGE and western blot analysis

To collect parasite proteins, iRBCs were lysed with 5% saponin on ice. Parasites were washed with PBSx1 and re-suspended with 2 $\times$  Laemmli sample buffer (Sigma). Proteins were loaded on 4–20% polyacrylamide gels (Bio-Rad) along with protein size marker (Precision plus, Bio-Rad) and were subjected to SDS-PAGE at 100 volts for 1 hour. Proteins were electroblotted to nitrocellulose membrane (Schleicher & Schuell BioScience) using a wet transfer apparatus (Bio-Rad) at 135 mA for 90 minutes. Membranes were blocked with 5% skim milk (Difco) in PBST for 1 hour at RT. Immunodetection was carried out by incubating the membrane with a primary antibody diluted with blocking solution as follows:

1/700 Mouse  $\alpha$ -HA (Roche), 1/500 rabbit  $\alpha$ -Pf39 (MR4), 1/500 rabbit  $\alpha$ -H3K9me3 (07442, Millipore), 1/500 rabbit  $\alpha$ -GFP (Roche) and 1:1000 rabbit  $\alpha$ -aldolase (polyclonal, kindly given by Dr Jake Baum, WEHI) followed by incubation with rabbit  $\alpha$ -mouse or mouse  $\alpha$ -rabbit secondary antibodies conjugated to Horseradish Peroxidase (HRP) (Jackson, ImmunoResearch Laboratories, INC). Membranes were developed by EZ/ECL solution (Israel Biological Industries, LTD).

#### Plasmid construction

*PfSec13* was cloned into the expression vector pHRIDH (Li et al., 2008) fused to GFP at its C-terminus to generate pH-sec13GFP-IDH. GFP was amplified using the primers GPPF-GFPR (F-gaagatctagtagtaaggagaagaact; R-ccaagctttttatgtat-agttcatccat) and cloned using *Bgl*III and *Hind*III. *PfSec13* was amplified using the primers PfSec13F and PfSec13R (F-ccccgggaaatgaacgaattagtagtg; R-ccccgggattggtcatatgtatt) and cloned into the pHRIDH plasmid using *Xma*I. To tag the endogenous PfSec13 with an HA epitope, *PfSec13* 3' was amplified using the primers PfSec133'F-PfSec133'R (F-aactgcagcctccagcacaacaacaag; R-catgcatggattggtcatatgtattttt) and cloned into the plasmid pH005-3 $\times$ HA (Flueck et al., 2010) using *Pst*I and *Nco*I. Integration into the genome occurred in a single crossover recombination following cycles of "on" and "off" drug selection with 5 nM WR99210. PCR across integration site was done using a primer on the endogenous PfSec13 fragment and a primer at the HA tag (F-GCGCCTCGAGCTGGTCA-AATGAACGG; R-AAGCTTTTAGAGCTCGGCATAATCTGGAAC).

#### Southern blot analysis

Analysis of the integrated construct was performed using Southern blots and diagnostic PCR crossing the integration sites followed by sequencing. Southern blots were performed according to established protocols (Sambrook et al., 1989). Briefly, genomic DNA isolated from recombinant parasites was digested to completion by the restriction enzyme *Sac*I and subjected to gel electrophoresis using 1% agarose in Tris/borate/EDTA (TBE). The DNA was transferred to high-bond nitrocellulose membrane by capillary action after alkaline denaturation. DNA detection was performed using DIG High Prime DNA Labeling and Detection starter kit (Roche). The 3' end of PfSec13 was cut with *Nco*I-*Pst*I from the p005-Sec13 construct and was used as a probe.

#### Chromatin IP

ChIPs were carried out using 1% formaldehyde crosslinked chromatin as described before (Chookajorn et al., 2007) with slight modifications. Crosslinking was halted by addition of Glycine to a 0.125 M final concentration. Sonication was carried out by the Bioruptor<sup>®</sup>Plus (diagenode) for 12 pulses to get a DNA size range of 100–800 bp. Sonicated chromatin was incubated with 1  $\mu$ g antibody [ $\alpha$ -HA 3F10 (Roche);  $\alpha$ -GFP (AbCam)] in presence of 30  $\mu$ l A/G Sepharose beads (Santa Cruz Biotechnology) overnight at 4°C. The sample was thoroughly washed and bound chromatin was eluted by incubating the sample with elution buffer (50 mM Tris-Cl, 10 mM EDTA, 1% SDS and 5 mM DTT) for 15 min at 65°C. The bound fraction was decrosslinked by incubation over night at 65°C. The decrosslinked sample was incubated with 20  $\mu$ g Glycogen and 100  $\mu$ g Proteinase K for 1 hr at 65°C. DNA was purified using PCR purification columns (Qiagen). The efficiency of ChIP at each specific genomic locus was tested by quantitative real time PCR (Corbett 6000) using primer sets as described before (Flueck et al., 2010; Chookajorn et al., 2007). The amount of target DNA recovered after immunoprecipitation was directly compared to a ten-fold dilution series of input DNA, and defined as percentage of input for each locus.

#### Co-IP

A 300 ml portion of either Sec13-HA transgenic line or NF54 wild-type parasite cultures at 7% parasitemia was lysed on ice using 0.05% saponin. The parasite pellet was washed twice with 5 ml iced cold 1 $\times$  PBS and was then incubated with 3 ml of cold IP buffer [0.5% Tx-100 in 1 $\times$  PBS, 1 $\times$  Complete EDTA free Protease inhibitor (Roche)] for 20 min on ice. To discard cell debris, the extract was centrifuged at 3000 rpm for 3 min at 4°C. The supernatant was incubated with 30  $\mu$ l bed volume of  $\alpha$ -HA bound agarose beads (Abcam) that were prewashed with low pH buffer (50 mM glycine, 0.5M NaCl pH 3) for the removal of unbound antibodies followed by a neutralizing high pH wash (50 mM Tris HCl, 0.5M NaCl pH 8). The parasites extracts were incubated with the beads for 2 hrs at 4°C while swirling. Then loaded on a 1.5 ml spin column (BioRad) and flew through by gravity. The unbound fraction was collected and kept in -20°C. The agarose beads left on the columns were washed five times by gravity flow with 500  $\mu$ l of the IP buffer and twice with 500  $\mu$ l 1 $\times$  PBS. The beads were then incubated with warm 150  $\mu$ l of non reducing sample buffer (4% SDS, 100 mM Tris-HCl, pH 8) for 5 min and eluted into a clean tube.

#### Mass spectrometry analysis

The samples for the LC-MS/MS analyses were prepared by loading the bound fraction of the PfSec13-HA pull down and the NF54 control pull down on a 4–20% acrylamide gel (BioRad) and run on gel until the samples reached a distance of 1.5 cm from the bottom of the loading wells. Then the gels were washed twice

with water and stained with 100 ml SeeBand protein staining solution (Geba) for 1 hour at RT while swirling. The stain was then washed with water for 30 min and the stained samples were cut out and sent for Mass spectrometry analyses. The samples were trypsinized and the tryptic peptides were analyzed by LC-MS/MS on the OrbitrapXL (Thermo) mass spectrometer and identified by Discoverer software version 1.3 against the *Plasmodium* section of the NCBI-NR database and against decoy databases (in order to determine the false discovery rate (FDR), using the Sequest and the Mascot search engine. Proteins that were enriched at least twice in the PfSec13-HA pull down comparing with the control and in which at least three peptides were identified are presented.

#### Downregulation of PfSec13 using specific PNA molecules

PfSec13-HA transgenic line and NF54-luc parasites (Salazar et al., 2012) were incubated for 24 hours with either specific PfSec13PNA molecule [5' COOH-(K)<sub>8</sub> TGGATAGT(TO)CCTTCTAG] or non-specific PNA molecule [5' COOH-(K)<sub>8</sub> TCTAGACCT(TO)ATGCAGC(TR)]. These parasite lines enabled to measure the level of downregulation in the expression of the endogenous PfSec13 protein by western blot using  $\alpha$ -HA antibody and to perform luciferase assays to measure parasites' viability as described (Salazar et al., 2012). After 24 h of incubation the culture medium was changed daily and PNA molecules were washed away. Parasitemia was also counted by direct microscopy on Giemsa stained slides.

#### Acknowledgements

We would like to thank Dr. Till Voss from The University of Basel for kindly providing us with the PfHP1 expression vector and the pH005-3 $\times$ HA plasmid used as a template for cloning. We thank Dr. Susann Herrmann from McMaster University for the GRASP-mCherry expression vector. We also thank David Riglar and Elizabeth Zuccala for their help in establishing synchronization and microscopy techniques.

#### Author contributions

N.D.-P. and R.D. conceived, designed and performed experiments and interpreted results. A.N., N.K., M.P., V.S., L.T. and C.B.W. participated in experiments. W.W. analyzed data and interpreted results. M.E., E.Y. and J.B. designed experiments and interpreted results. T.W.G. provided new reagents, designed experiments and interpreted results. N.D.-P. and R.D. wrote the paper.

#### Funding

This work was supported by the United States-Israel Binational Science Foundation [grant number 2007350]. R.D. is also supported by the Jacob and Lena Joels Memorial Foundation Senior Lectureship for Excellence in the Life and Medical Sciences. N.D.-P. was supported by an Australia-Israel Scientific Exchange Foundation (AISEF) student fellowship and a scholarship from the Australian Friends of the Hebrew University, Jerusalem. L.T. is supported by a Chancellor's Postdoctoral Fellowship from the University of Technology, Sydney. C.B.W. is supported by a Senior Research Fellowship from the National Health and Medical Research Council of Australia (NHMRC). Research in the Baum laboratory was supported through an NHMRC Project Grant [grant number APP1024678] and a Human Frontier Science Program Young Investigator Program Grant [grant number RGY0071/2011]. W.W. is supported through an NHMRC Early Career Fellowship [grant number APP1053801]. J.B. is supported through an Australian Research Council (ARC) Future Fellowship [grant number FT100100112]. Experimental data presented here was made possible through Victorian State Government Operational Infrastructure Support and the Australian Government NHMRC Independent Research Institutes Infrastructure Support Scheme (IRIIS).

Supplementary material available online at

<http://jcs.biologists.org/lookup/suppl/doi:10.1242/jcs.122119/-/DC1>

#### References

Akhtar, A. and Gasser, S. M. (2007). The nuclear envelope and transcriptional control. *Nat. Rev. Genet.* **8**, 507–517.

- Angrisano, F., Riglar, D. T., Sturm, A., Volz, J. C., Delves, M. J., Zuccala, E. S., Turnbull, L., Dekiwadia, C., Olshina, M. A., Marapana, D. S. et al. (2012). Spatial localisation of actin filaments across developmental stages of the malaria parasite. *PLoS ONE* **7**, e32188.
- Aregawi, M., Cibulskis, R. E., Kita, Y., Otten, M., Williams, R.; World Health Organization. Global Malaria Programme. (2010). *World Malaria Report 2010*. Geneva: World Health Organisation.
- Arib, G. and Akhtar, A. (2011). Multiple facets of nuclear periphery in gene expression control. *Curr. Opin. Cell Biol.* **23**, 346-353.
- Baum, J., Papenfuss, A. T., Mair, G. R., Janse, C. J., Vlachou, D., Waters, A. P., Cowman, A. F., Crabb, B. S. and de Koning-Ward, T. F. (2009). Molecular genetics and comparative genomics reveal RNAi is not functional in malaria parasites. *Nucleic Acids Res.* **37**, 3788-3798.
- Blobel, G. (1985). Gene gating: a hypothesis. *Proc. Natl. Acad. Sci. USA* **82**, 8527-8529.
- Boyle, M. J., Wilson, D. W., Richards, J. S., Riglar, D. T., Tetteh, K. K., Conway, D. J., Ralph, S. A., Baum, J. and Beeson, J. G. (2010). Isolation of viable Plasmodium falciparum merozoites to define erythrocyte invasion events and advance vaccine and drug development. *Proc. Natl. Acad. Sci. USA* **107**, 14378-14383.
- Brickner, J. H. and Walter, P. (2004). Gene recruitment of the activated INO1 locus to the nuclear membrane. *PLoS Biol.* **2**, e342.
- Brohawn, S. G. and Schwartz, T. U. (2009). Molecular architecture of the Nup84-Nup145C-Sec13 edge element in the nuclear pore complex lattice. *Nat. Struct. Mol. Biol.* **16**, 1173-1177.
- Bucci, M. and Wente, S. R. (1997). In vivo dynamics of nuclear pore complexes in yeast. *J. Cell Biol.* **136**, 1185-1199.
- Cabal, G. G., Genovesio, A., Rodríguez-Navarro, S., Zimmer, C., Gadal, O., Lesne, A., Buc, H., Feuerbach-Fournier, F., Olivo-Marin, J. C., Hurt, E. C. et al. (2006). SAGA interacting factors confine sub-diffusion of transcribed genes to the nuclear envelope. *Nature* **441**, 770-773.
- Capelson, M. and Hetzer, M. W. (2009). The role of nuclear pores in gene regulation, development and disease. *EMBO Rep.* **10**, 697-705.
- Capelson, M., Doucet, C. and Hetzer, M. W. (2010a). Nuclear pore complexes: guardians of the nuclear genome. *Cold Spring Harb. Symp. Quant. Biol.* **75**, 585-597.
- Capelson, M., Liang, Y., Schulte, R., Mair, W., Wagner, U. and Hetzer, M. W. (2010b). Chromatin-bound nuclear pore components regulate gene expression in higher eukaryotes. *Cell* **140**, 372-383.
- Casolari, J. M., Brown, C. R., Drubin, D. A., Rando, O. J. and Silver, P. A. (2005). Developmentally induced changes in transcriptional program alter spatial organization across chromosomes. *Genes Dev.* **19**, 1188-1198.
- Chakalova, L., Debrand, E., Mitchell, J. A., Osborne, C. S. and Fraser, P. (2005). Replication and transcription: shaping the landscape of the genome. *Nat. Rev. Genet.* **6**, 669-677.
- Chenna, R., Sugawara, H., Koike, T., Lopez, R., Gibson, T. J., Higgins, D. G. and Thompson, J. D. (2003). Multiple sequence alignment with the Clustal series of programs. *Nucleic Acids Res.* **31**, 3497-3500.
- Chookajorn, T., Dzikowski, R., Frank, M., Li, F., Jiwani, A. Z., Hartl, D. L. and Deitsch, K. W. (2007). Epigenetic memory at malaria virulence genes. *Proc. Natl. Acad. Sci. USA* **104**, 899-902.
- Colón-Ramos, D. A., Salisbury, J. L., Sanders, M. A., Shenoy, S. M., Singer, R. H. and García-Blanco, M. A. (2003). Asymmetric distribution of nuclear pore complexes and the cytoplasmic localization of beta2-tubulin mRNA in Chlamydomonas reinhardtii. *Dev. Cell* **4**, 941-952.
- D'Angelo, M. A. and Hetzer, M. W. (2006). The role of the nuclear envelope in cellular organization. *Cell. Mol. Life Sci.* **63**, 316-332.
- Daigle, N., Beaudouin, J., Hartnell, L., Imreh, G., Hallberg, E., Lippincott-Schwartz, J. and Ellenberg, J. (2001). Nuclear pore complexes form immobile networks and have a very low turnover in live mammalian cells. *J. Cell Biol.* **154**, 71-84.
- DeGrasse, J. A., Chait, B. T., Field, M. C. and Rout, M. P. (2008). High-yield isolation and subcellular proteomic characterization of nuclear and subnuclear structures from trypanosomes. *Methods Mol. Biol.* **463**, 77-92.
- Dieppois, G., Iglesias, N. and Stutz, F. (2006). Cotranscriptional recruitment to the mRNA export receptor Mex67p contributes to nuclear pore anchoring of activated genes. *Mol. Cell Biol.* **26**, 7858-7870.
- Dilworth, D. J., Tackett, A. J., Rogers, R. S., Yi, E. C., Christmas, R. H., Smith, J. J., Siegel, A. F., Chait, B. T., Wozniak, R. W. and Aitchison, J. D. (2005). The mobile nucleoporin Nup2p and chromatin-bound Prp20p function in endogenous NPC-mediated transcriptional control. *J. Cell Biol.* **171**, 955-965.
- Duraisingh, M. T., Voss, T. S., Marty, A. J., Duffy, M. F., Good, R. T., Thompson, J. K., Freitas-Junior, L. H., Scherf, A., Crabb, B. S. and Cowman, A. F. (2005). Heterochromatin silencing and locus repositioning linked to regulation of virulence genes in Plasmodium falciparum. *Cell* **121**, 13-24.
- Dzikowski, R., Frank, M. and Deitsch, K. (2006). Mutually exclusive expression of virulence genes by malaria parasites is regulated independently of antigen production. *PLoS Pathog.* **2**, e22.
- Dzikowski, R., Li, F., Amulic, B., Eisberg, A., Frank, M., Patel, S., Wellems, T. E. and Deitsch, K. W. (2007). Mechanisms underlying mutually exclusive expression of virulence genes by malaria parasites. *EMBO Rep.* **8**, 959-965.
- Egociglu, D. and Brickner, J. H. (2011). Gene positioning and expression. *Curr. Opin. Cell Biol.* **23**, 338-345.
- Enninga, J., Levy, D. E., Blobel, G. and Fontoura, B. M. (2002). Role of nucleoporin induction in releasing an mRNA nuclear export block. *Science* **295**, 1523-1525.
- Enninga, J., Levy, A. and Fontoura, B. M. (2003). Sec13 shuttles between the nucleus and the cytoplasm and stably interacts with Nup96 at the nuclear pore complex. *Mol. Cell Biol.* **23**, 7271-7284.
- Fiserova, J., Kiseleva, E. and Goldberg, M. W. (2009). Nuclear envelope and nuclear pore complex structure and organization in tobacco BY-2 cells. *Plant J.* **59**, 243-255.
- Flueck, C., Bartfai, R., Volz, J., Niederwieser, I., Salcedo-Amaya, A. M., Alako, B. T., Ehlgren, F., Ralph, S. A., Cowman, A. F., Bozdech, Z. et al. (2009). Plasmodium falciparum heterochromatin protein 1 marks genomic loci linked to phenotypic variation of exported virulence factors. *PLoS Pathog.* **5**, e1000569.
- Flueck, C., Bartfai, R., Niederwieser, I., Witmer, K., Alako, B. T., Moes, S., Bozdech, Z., Jenoe, P., Stunnenberg, H. G. and Voss, T. S. (2010). A major role for the Plasmodium falciparum ApiAP2 protein PfSIP2 in chromosome end biology. *PLoS Pathog.* **6**, e1000784.
- Fowler, R. E., Smith, A. M., Whitehorn, J., Williams, I. T., Bannister, L. H. and Mitchell, G. H. (2001). Microtubule associated motor proteins of Plasmodium falciparum merozoites. *Mol. Biochem. Parasitol.* **117**, 187-200.
- Freitas-Junior, L. H., Bottius, E., Pirrit, L. A., Deitsch, K. W., Scheidig, C., Guinet, F., Nehrbass, U., Wellems, T. E. and Scherf, A. (2000). Frequent ectopic recombination of virulence factor genes in telomeric chromosome clusters of P. falciparum. *Nature* **407**, 1018-1022.
- Freitas-Junior, L. H., Hernandez-Rivas, R., Ralph, S. A., Montiel-Condado, D., Ruvalcaba-Salazar, O. K., Rojas-Meza, A. P., Mancio-Silva, L., Leal-Silvestre, R. J., Gontijo, A. M., Shorte, S. et al. (2005). Telomeric heterochromatin propagation and histone acetylation control mutually exclusive expression of antigenic variation genes in malaria parasites. *Cell* **121**, 25-36.
- Giaever, G., Chu, A. M., Ni, L., Connelly, C., Riles, L., Véronneau, S., Dow, S., Lucau-Danila, A., Anderson, K., André, B. et al. (2002). Functional profiling of the Saccharomyces cerevisiae genome. *Nature* **418**, 387-391.
- Gouet, P., Courcelle, E., Stuart, D. I. and Métoz, F. (1999). ESPript: analysis of multiple sequence alignments in PostScript. *Bioinformatics* **15**, 305-308.
- Griffis, E. R., Altan, N., Lippincott-Schwartz, J. and Powers, M. A. (2002). Nup98 is a mobile nucleoporin with transcription-dependent dynamics. *Mol. Biol. Cell* **13**, 1282-1297.
- Grossman, E., Medalia, O. and Zwerger, M. (2012). Functional architecture of the nuclear pore complex. *Annu. Rev. Biophys.* **41**, 557-584.
- Ho, H. C. (2010). Redistribution of nuclear pores during formation of the redundant nuclear envelope in mouse spermatids. *J. Anat.* **216**, 525-532.
- Hoelz, A., Debler, E. W. and Blobel, G. (2011). The structure of the nuclear pore complex. *Annu. Rev. Biochem.* **80**, 613-643.
- Howitt, C. A., Wilinski, D., Llinás, M., Templeton, T. J., Dzikowski, R. and Deitsch, K. W. (2009). Clonally variant gene families in Plasmodium falciparum share a common activation factor. *Mol. Microbiol.* **73**, 1171-1185.
- Ishii, K., Arib, G., Lin, C., Van Houwe, G. and Laemmli, U. K. (2002). Chromatin boundaries in budding yeast: the nuclear pore connection. *Cell* **109**, 551-562.
- Joergensen, L., Bengtsson, D. C., Bengtsson, A., Ronander, E., Berger, S. S., Turner, L., Dalgaard, M. B., Cham, G. K., Victor, M. E., Lavstsen, T. et al. (2010). Surface co-expression of two different PfEMP1 antigens on single plasmodium falciparum-infected erythrocytes facilitates binding to ICAM1 and PECAM1. *PLoS Pathog.* **6**, e1001083.
- Kalverda, B., Pickersgill, H., Shloma, V. V. and Fornerod, M. (2010). Nucleoporins directly stimulate expression of developmental and cell-cycle genes inside the nucleoplasm. *Cell* **140**, 360-371.
- Kobylnski, K. C., Foy, B. D. and Richardson, J. H. (2012). Ivermectin inhibits the sporogony of Plasmodium falciparum in Anopheles gambiae. *Malar. J.* **11**, 381.
- Köhler, A. and Hurt, E. (2010). Gene regulation by nucleoporins and links to cancer. *Mol. Cell* **38**, 6-15.
- Li, F., Sonbuchner, L., Kyes, S. A., Epp, C. and Deitsch, K. W. (2008). Nuclear non-coding RNAs are transcribed from the centromeres of Plasmodium falciparum and are associated with centromeric chromatin. *J. Biol. Chem.* **283**, 5692-5698.
- Lindsay, M. E., Plafker, K., Smith, A. E., Clurman, B. E. and Macara, I. G. (2002). Np60/Nup50 is a tri-stable switch that stimulates importin-alpha:beta-mediated nuclear protein import. *Cell* **110**, 349-360.
- Lopez-Rubio, J. J., Mancio-Silva, L. and Scherf, A. (2009). Genome-wide analysis of heterochromatin associates clonally variant gene regulation with perinuclear repressive centers in malaria parasites. *Cell Host Microbe* **5**, 179-190.
- Maeshima, K., Yahata, K., Sasaki, Y., Nakatomi, R., Tachibana, T., Hashikawa, T., Imamoto, F. and Imamoto, N. (2006). Cell-cycle-dependent dynamics of nuclear pores: pore-free islands and lamins. *J. Cell Sci.* **119**, 4442-4451.
- Oehring, S. C., Woodcroft, B. J., Moes, S., Wetzel, J., Dietz, O., Pulfer, A., Dekiwadia, C., Maeser, P., Flueck, C., Witmer, K. et al. (2012). Organellar proteomics reveals hundreds of novel nuclear proteins in the malaria parasite Plasmodium falciparum. *Genome Biol.* **13**, R108.
- Pérez-Toledo, K., Rojas-Meza, A. P., Mancio-Silva, L., Hernández-Cuevas, N. A., Delgado, D. M., Vargas, M., Martínez-Calvillo, S., Scherf, A. and Hernandez-Rivas, R. (2009). Plasmodium falciparum heterochromatin protein 1 binds to tri-methylated histone 3 lysine 9 and is linked to mutually exclusive expression of var genes. *Nucleic Acids Res.* **37**, 2596-2606.
- Powers, M. A., Macaulay, C., Masiarz, F. R. and Forbes, D. J. (1995). Reconstituted nuclei depleted of a vertebrate GLFG nuclear pore protein, p97, import but are defective in nuclear growth and replication. *J. Cell Biol.* **128**, 721-736.
- Rabut, G., Lénárt, P. and Ellenberg, J. (2004). Dynamics of nuclear pore complex organization through the cell cycle. *Curr. Opin. Cell Biol.* **16**, 314-321.

- Ralph, S. A., Scheidig-Benatar, C. and Scherf, A. (2005). Antigenic variation in Plasmodium falciparum is associated with movement of var loci between subnuclear locations. *Proc. Natl. Acad. Sci. USA* **102**, 5414-5419.
- Riglar, D. T., Richard, D., Wilson, D. W., Boyle, M. J., Dekiwadia, C., Turnbull, L., Angrisano, F., Marapana, D. S., Rogers, K. L., Whitchurch, C. B. et al. (2011). Super-resolution dissection of coordinated events during malaria parasite invasion of the human erythrocyte. *Cell Host Microbe* **9**, 9-20.
- Roy, A., Kucukural, A. and Zhang, Y. (2010). I-TASSER: a unified platform for automated protein structure and function prediction. *Nat. Protoc.* **5**, 725-738.
- Salazar, E., Bank, E. M., Ramsey, N., Hess, K. C., Deitsch, K. W., Levin, L. R. and Buck, J. (2012). Characterization of Plasmodium falciparum adenyllyl cyclase- $\beta$  and its role in erythrocytic stage parasites. *PLoS ONE* **7**, e39769.
- Salcedo-Amaya, A. M., van Driel, M. A., Alako, B. T., Trelle, M. B., van den Elzen, A. M., Cohen, A. M., Janssen-Megens, E. M., van de Vegte-Bolmer, M., Selzer, R. R., Iniguez, A. L. et al. (2009). Dynamic histone H3 epigenome marking during the intraerythrocytic cycle of Plasmodium falciparum. *Proc. Natl. Acad. Sci. USA* **106**, 9655-9660.
- Salcedo-Amaya, A. M., Hoesjmakers, W. A., Bártfai, R. and Stunnenberg, H. G. (2010). Malaria: could its unusual epigenome be the weak spot? *Int. J. Biochem. Cell Biol.* **42**, 781-784.
- Sambrook, J., Fritsch, E. and Maniatis, T. (1989). *Molecular Cloning: A Laboratory Manual*. New York: Cold Spring Harbor Laboratory.
- Schmid, M., Arib, G., Laemmli, C., Nishikawa, J., Durussel, T. and Laemmli, U. K. (2006). Nup-PI: the nucleopore-promoter interaction of genes in yeast. *Mol. Cell* **21**, 379-391.
- Schrével, J., Asfaux-Foucher, G. and Bafort, J. M. (1977). [Ultrastructural study of multiple mitoses during sporogony of Plasmodium b. berghei]. *J. Ultrastruct. Res.* **59**, 332-350.
- Siniosoglou, S., Wimmer, C., Rieger, M., Doye, V., Tekotte, H., Weise, C., Emig, S., Segref, A. and Hurt, E. C. (1996). A novel complex of nucleoporins, which includes Sec13p and a Sec13p homolog, is essential for normal nuclear pores. *Cell* **84**, 265-275.
- Siniosoglou, S., Lutzmann, M., Santos-Rosa, H., Leonard, K., Mueller, S., Aebi, U. and Hurt, E. (2000). Structure and assembly of the Nup84p complex. *J. Cell Biol.* **149**, 41-54.
- Smitherman, M., Lee, K., Swanger, J., Kapur, R. and Clurman, B. E. (2000). Characterization and targeted disruption of murine Nup50, a p27(Kip1)-interacting component of the nuclear pore complex. *Mol. Cell Biol.* **20**, 5631-5642.
- Stagg, S. M., Gürkan, C., Fowler, D. M., LaPointe, P., Foss, T. R., Potter, C. S., Carragher, B. and Balch, W. E. (2006). Structure of the Sec13/31 COPII coat cage. *Nature* **439**, 234-238.
- Steinberg, G., Schuster, M., Theisen, U., Kilaru, S., Forge, A. and Martin-Urdiroz, M. (2012). Motor-driven motility of fungal nuclear pores organizes chromosomes and fosters nucleocytoplasmic transport. *J. Cell Biol.* **198**, 343-355.
- Striepen, B., Jordan, C. N., Reiff, S. and van Dooren, G. G. (2007). Building the perfect parasite: cell division in apicomplexa. *PLoS Pathog.* **3**, e78.
- Struck, N. S., Herrmann, S., Schmuck-Barkmann, I., de Souza Dias, S., Haase, S., Cabrera, A. L., Treeck, M., Bruns, C., Langer, C., Cowman, A. F. et al. (2008a). Spatial dissection of the cis- and trans-Golgi compartments in the malaria parasite Plasmodium falciparum. *Mol. Microbiol.* **67**, 1320-1330.
- Struck, N. S., Herrmann, S., Langer, C., Krueger, A., Foth, B. J., Engelberg, K., Cabrera, A. L., Haase, S., Treeck, M. and Marti, M. (2008b). Plasmodium falciparum possesses two GRASP proteins that are differentially targeted to the Golgi complex via a higher- and lower-eukaryote-like mechanism. *J. Cell Sci.* **121**, 2123-2129.
- Taddei, A., Van Houwe, G., Hediger, F., Kalck, V., Cubizolles, F., Schober, H. and Gasser, S. M. (2006). Nuclear pore association confers optimal expression levels for an inducible yeast gene. *Nature* **441**, 774-778.
- Takizawa, T., Meaburn, K. J. and Misteli, T. (2008). The meaning of gene positioning. *Cell* **135**, 9-13.
- Tamura, K., Fukao, Y., Iwamoto, M., Haraguchi, T. and Hara-Nishimura, I. (2010). Identification and characterization of nuclear pore complex components in Arabidopsis thaliana. *Plant Cell* **22**, 4084-4097.
- Tan-Wong, S. M., Wijayatilake, H. D. and Proudfoot, N. J. (2009). Gene loops function to maintain transcriptional memory through interaction with the nuclear pore complex. *Genes Dev.* **23**, 2610-2624.
- Tokuyasu, K. T. (1986). Application of cryoultramicrotomy to immunocytochemistry. *J. Microsc.* **143**, 139-149.
- Trelle, M. B., Salcedo-Amaya, A. M., Cohen, A. M., Stunnenberg, H. G. and Jensen, O. N. (2009). Global histone analysis by mass spectrometry reveals a high content of acetylated lysine residues in the malaria parasite Plasmodium falciparum. *J. Proteome Res.* **8**, 3439-3450.
- Vaquerizas, J. M., Suyama, R., Kind, J., Miura, K., Luscombe, N. M. and Akhtar, A. (2010). Nuclear pore proteins nup153 and megator define transcriptionally active regions in the Drosophila genome. *PLoS Genet.* **6**, e1000846.
- Volz, J., Carvalho, T. G., Ralph, S. A., Gilson, P., Thompson, J., Tonkin, C. J., Langer, C., Crabb, B. S. and Cowman, A. F. (2010). Potential epigenetic regulatory proteins localise to distinct nuclear sub-compartments in Plasmodium falciparum. *Int. J. Parasitol.* **40**, 109-121.
- Volz, J. C., Bártfai, R., Petter, M., Langer, C., Josling, G. A., Tsuboi, T., Schwach, F., Baum, J., Rayner, J. C., Stunnenberg, H. G. et al. (2012). PSET10, a Plasmodium falciparum methyltransferase, maintains the active var gene in a poised state during parasite division. *Cell Host Microbe* **11**, 7-18.
- Voss, T. S., Healer, J., Marty, A. J., Duffy, M. F., Thompson, J. K., Beeson, J. G., Reeder, J. C., Crabb, B. S. and Cowman, A. F. (2006). A var gene promoter controls allelic exclusion of virulence genes in Plasmodium falciparum malaria. *Nature* **439**, 1004-1008.
- Wagstaff, K. M., Sivakumaran, H., Heaton, S. M., Harrich, D. and Jans, D. A. (2012). Ivermectin is a specific inhibitor of importin alpha/beta-mediated nuclear import able to inhibit replication of HIV-1 and dengue virus. *Biochem J.* **443**, 851-856.
- Wang, G. and Xu, X. S. (2004). Peptide nucleic acid (PNA) binding-mediated gene regulation. *Cell Res.* **14**, 111-116.
- Weiner, A., Dahan-Pasternak, N., Shimoni, E., Shinder, V., von Huth, P., Elbaum, M. and Dzikowski, R. (2011). 3D nuclear architecture reveals coupled cell cycle dynamics of chromatin and nuclear pores in the malaria parasite Plasmodium falciparum. *Cell. Microbiol.* **13**, 967-977.
- Winey, M., Yarar, D., Giddings, T. H., Jr and Mastronarde, D. N. (1997). Nuclear pore complex number and distribution throughout the Saccharomyces cerevisiae cell cycle by three-dimensional reconstruction from electron micrographs of nuclear envelopes. *Mol. Biol. Cell* **8**, 2119-2132.
- Yang, Z., Lasker, K., Schneidman-Duhovny, D., Webb, B., Huang, C. C., Pettersen, E. F., Goddard, T. D., Meng, E. C., Sali, A. and Ferrin, T. E. (2012). UCSF Chimera, MODELLER, and IMP: an integrated modeling system. *J. Struct. Biol.* **179**, 269-278.
- Zhang, Q., Huang, Y., Zhang, Y., Fang, X., Claes, A., Duchateau, M., Namane, A., Lopez-Rubio, J. J., Pan, W. and Scherf, A. (2011). A critical role of perinuclear filamentous actin in spatial repositioning and mutually exclusive expression of virulence genes in malaria parasites. *Cell Host Microbe* **10**, 451-463.
- Zimowska, G., Aris, J. P. and Paddy, M. R. (1997). A Drosophila Tpr protein homolog is localized both in the extrachromosomal channel network and to nuclear pore complexes. *J. Cell Sci.* **110**, 927-944.
- Zuleger, N., Robson, M. I. and Schirmer, E. C. (2011). The nuclear envelope as a chromatin organizer. *Nucleus* **2**, 339-349.